

FINAL REPORT SUBMITTED
TO
NATIONAL AERONAUTICS & SPACE ADMINISTRATION
MANNED SPACECRAFT CENTER
HOUSTON, TEXAS

on

CONTRACT #NASw-415
DEVELOPMENT OF A PERSONNEL DOSIMETRY SYSTEM
FOR APOLLO

FACILITY FORM 602

N 65 - 36 44 1
(ACCESSION NUMBER) (THRU)
39
(PAGES) (CODE)
RR - 65157
(NASA CR OR TMX OR AD NUMBER) (CATEGORY)
04

GPO PRICE \$ _____

CSFTI PRICE(S) \$ _____

Hard copy (HC) 2.00

Microfiche (MF) .50

ff 653 July 65

SOLID STATE RADIATIONS, INC.

FINAL REPORT SUBMITTED

TO

NATIONAL AERONAUTICS & SPACE ADMINISTRATION

MANNED SPACECRAFT CENTER

HOUSTON, TEXAS

on

CONTRACT #NASw-415

DEVELOPMENT OF A PERSONNEL DOSIMETRY SYSTEM FOR APOLLO

by

SOLID STATE RADIATIONS INC.

2261 South Carmelina Avenue

Los Angeles 64, California

FINAL REPORT ON
CONTRACT #NASW-415

for
DEVELOPMENT OF A PERSONNEL
DOSIMETRY SYSTEM FOR APOLLO

1. INTRODUCTION

The problem of accurately assessing the radiation dose to which the Apollo Astronauts are exposed resolves itself into two basic parts. The first aspect of the problem is a fundamental one, i.e. the evolution of a radiation dose measuring concept which will most accurately assess the hazard associated with radiation exposure without necessarily considering the limitations of size, weight, and power consumption which are imposed on equipment for manned spaceflight use. It is necessary to consider such an idealized measurement concept in order to accurately assess the limitations on real instruments which are capable of meeting the required engineering specifications. The second aspect of the problem is associated with these engineering limitations, i.e. preserving the maximum idealized performance in the face of extreme limitations on the amount and complexity of equipment which can be carried. These two aspects of the problem have been explored in the course of performance on the referenced contract, culminating in a subminiature dosimeter package with self-contained power and readout capable of indicating the dose delivered by fast protons and alpha particles, electrons, and to some extent, gamma rays with a resolution sufficient to provide information concerning the potential hazard associated with various parts of the mission. While some preliminary evaluation of the dosimetry packages has been performed, the most important task outstanding at the conclusion of this portion of the effort, is the evaluation of the dosimeter packages in a wide variety of radiation environments, the resolution of certain anomalies in the calibrations performed and the completion of environmental testing procedures for the generation of flight hardware.

2. CONSIDERATION OF THE DOSIMETRY PROBLEM

The biological effects of ionizing radiation have been extensively studied with a view to establishing permissible exposures. Since, as is the case with most biological phenomena, the effects are statistical in nature and the experience with the exposure of human beings to ionizing radiation is necessarily limited, a considerable element of uncertainty necessarily exists in the specifying of a single tolerance dose which may not be exceeded without damage. However, certain general concepts have come to be accepted which must be used, for lack of better information, by the instrument designer in attempting to arrive at a proper instrument concept. To briefly summarize these, there are three major factors which contribute to the potential hazard of exposure to ionizing radiation. These are (1) the radiation dose expressed in terms of energy deposited by the ionizing radiation; (2) the location of the energy deposition in the body; and (3) the relative biological effectiveness of this particular type of radiation in damaging of living organisms.

The measurement of radiation dose was originally performed by means of air wall ionization chambers, resulting in the establishment of the roentgen as the basic unit of radiation dose as that amount of X or gamma radiation such that the associated corpuscular emission/0.0012393 gram of air produces in air ions carrying 1 esu of charge of either sign. In order to generalize this concept to include dose in other media, at the 1953 Copenhagen meeting of the International Commission on Radiological Units, the rad was chosen as the unit of absorbed dose and defined as the intensity of ionizing radiation resulting in the deposition of 100 ergs/gram of any medium. It is of course necessary to specify the medium under consideration and as the result of the difference in the interaction of radiation with materials of different atomic composition, the dose in rads of a given radiation field will vary somewhat depending on the substance used as a reference. For biological purposes, the rad dose to soft tissue is generally considered composed approximately of 75% oxygen, 12% carbon, 10% hydrogen and 4% nitrogen by weight. In order to provide a relationship with older units, the roentgen equivalent physical or rep is defined as the amount of radiation corresponding to the absorption of 93 ergs/gram of soft tissue of that composition.

The point of deposition of dose has a profound effect on the potential biological hazard. Specific sites in the human body vary tremendously in

their sensitivity to radiation. In general the most radiation sensitive sites tend to be located at least several centimeters below the surface of the skin including the bone marrow and the abdominal organs. Skin, fat and muscle are somewhat less susceptible to damage by radiation. An exception to this situation exists with regard to the eye. The cornea of the eye has shown to be extremely radiation sensitive, radiation induced cataracts having been observed as the only long term consequence of accidental radiation exposures particularly to heavy ionizing particles such as protons and alpha particles. The site of deposition of radiation is also important because of the phenomenon of build up. This results from the production of secondary radiation following the initial interaction of radiation with matter. In the case of gamma rays, build up occurs from secondary X-rays produced by Compton interactions, annihilation quanta resulting from pair production and in the case of charged particles from direct nuclear reactions. Thus in some cases the depth dose will considerably exceed the surface dose due to build up while for other types of radiation the reverse can be true due to shielding.

When considering a wide variety of types of ionizing radiation, the problem of relative biological effectiveness becomes increasingly difficult. For a particular type of radiation, rbe is defined as the ratio between the dose in rads of gamma radiation from a Co^{60} source to produce a given biological change, to the dose in rads of radiation under comparison to produce the same biological change. For the purposes of radiological protection, the simplification is frequently made that rbe is equal to 1 for X, gamma and beta radiation, is equal to 10 for protons, fast neutrons and alpha particles, is equal to 20 for ions of mass greater than 4. While for ordinary radiological protection purposes such assumptions may be adequate, they cannot be considered sufficiently accurate for making of judgements in marginal cases.

A more precise measure of rbe has been made by relating rbe to the energy loss/unit path length of the secondary ionizing radiation known as LET or linear energy transfer. This concept arises from the view that the damage to an individual cell has a threshold of energy and thus the probability of destruction of the cell depends on the probability that this threshold

exceeded. Clearly, as the rate of energy deposition of the primary and secondary radiations increases, this probability for biological damage in a given cell increases. In principle then, rbe should be estimated by determining the spectrum of LET resulting from the interaction of the radiation with tissue. Experimental measurement of the LET spectrum has been performed in a laboratory using proportional counters of a highly specialized design. While this work is still experimental, it appears to have promise in arriving at a more precise statement of the rbe for different radiations.

The dosimetry problem for manned space travel involves a description of the radiation field with regard to physical dose, at biologically significant depths with the appropriate rbe factors applied for the different types of radiation encountered. Extensive studies have been performed on the sources of possible radiation dose in a manned space mission with the general conclusion that the most significant dose contribution in space results from high energy solar protons in the event of solar flares. Because of the high rbe of such particles, this source of dose should be most precisely characterized. In addition, trapped electrons and bremsstrahlung associated with stopping of these electrons in the material of the spacecraft can represent a significant contribution to dose particularly if rendezvous operations in the region of the belts takes considerable time, although the estimated dose for types of missions planned is quite small. A third possible source of radiation dose comes from beta and gamma emitters on the surface of the moon created by bombardment of the moon surface by protons. While the dose contribution from this source has not been experimentally verified, preliminary estimates indicate that it will be relatively low. However, it cannot be discounted altogether. The Apollo radiation dosimetry then is to be regarded primarily as a proton dosimeter and such has been the philosophy pursued in its design. However, preservation of response to electrons and photons is valuable in increasing the universality of the instrument.

3. DISCUSSION OF DESIGN CONSTRAINTS

In order that a personnel dosimetry system perform its function in space, certain constraints must be imposed on it as opposed to a laboratory system for making the same measurement. (1) It must be capable of being carried on the person of the astronaut without encumbering his ability to perform required tasks. (2) It should provide information on a current basis with regard to the radiation safety status of the mission. (3) It should be capable of functioning in the same environment that the astronaut will encounter both inside the spacecraft and on the surface of the moon. (4) It must provide data which is readily interpreted in terms of immediate or potential radiation hazard including some indication of rate as well as total dose. A number of instrument concepts were evaluated in the course of the present development with a view toward creating an instrument within these constraints. While a detailed account of the various alternatives will not be given, a few of the detailed constraints should be explored in order to guide the reader into a better understanding of the rationale of the instrument developed. An ideal dose measuring instrument would be one in which the sensor was in contact with the radiation sensitive structures in such a way that it would sample the radiation environment with the greatest possible accuracy. Toward this end, the early phase of the program for the investigation of dosimetry techniques in space was devoted to the development of various in-vivo radiation detectors. While these are of interest for medical research activities, and possible animal space experiments, it is clearly impractical to consider the implantation of radiation sensors in the bodies of the astronauts. Even the most pessimistic estimates of the radiation hazard, do not place it sufficiently high to justify the discomfort and potential danger of in-vivo sensors of radiation. For this reason, the placement of the radiation sensors must necessarily be compromised by a location on or near the surface of the body. A possible concept was evolved wherein the sensors might be located near or in contact with the skin with a remote readout available. Such a concept however, would require penetrating the pressure integrity of the space suit by the electrical leads necessary to communicate signals from a sensor located within the space suit to a readout located outside. As all such penetrations of the space suit represent

not only severe engineering liaison problems, but potential hazards to the pressure integrity of the suit, a decision was made to locate all elements of the dosimeter package outside the pressurized suit. Of all possible concepts, a self-contained package to be located in a pocket on the outside of the space suit in the region of the abdomen or thighs appeared to be most convenient while still maintaining reasonable elements of good personal dosimetry concept. While the outside environment is quite hostile in terms of temperature extremes to electronic instrumentation of all sorts, it was felt possible to moderate the environment by good thermal contact between the dosimetry package and the space suit itself. This tends to severely limit the size and weight of the instrument since it clearly should not interfere with the free movement of the astronaut in any way. It was agreed that these conditions could be fulfilled by a package approximately 1" x 2" x 3" provided it was carefully designed to be free of any sharp corners or projections which might represent a source of damage to the space suit. Because of the requirement for free movement of the astronaut, particularly in connection with movement on the surface of the moon, the dosimetry system should be completely independent of the spacecraft with regard to power and readout provisions. This limitation then required a power system and readout provision which could be packaged in the allotted space while still providing power and provision for readout for the entire duration of the mission. It will be clear that these requirements have imposed certain limitations on a dosimetry system. However, the advantages of flexibility of use gained would appear to outweigh any disadvantages introduced.

4. GENERAL SYSTEM DESIGN

A basic dosimetry system consists of a detector responsive to ionizing radiation, an electronic system capable of converting the signals from the detector into some quantity proportional to dose, a readout system capable of displaying the accumulated dose, and a power source to provide energy for the other components. The two aspects of the system which interface with the outside world, the detector and the readout, tend to dictate the over-all system design. In both cases, the extreme requirements for size and power consumption have severely limited the available choices. A conventional gas ionization chamber is clearly not applicable. Even for chambers operated at high pressure, the available chamber volume is so small as to reduce the amount of observed charge below the reasonable threshold of observation. Gas proportional counters are little better. While considerable gain is available in the gas amplification process, the stability of such devices particularly in the small size necessary is extremely questionable. The logical choice is the semiconductor radiation detector, since this represents the highest density device capable of producing electrical charge proportional to energy absorbed from radiation fields. In order to reduce, insofar as possible, directional effects and to simulate as nearly as possible the dose produced in tissue, a small cubic detector embedded in a tissue equivalent medium is employed. The size of the detector is dictated by the conflicting dosimetry requirements that, on one hand, the presence of the silicon perturb the tissue equivalent environment as little as possible, and on the other hand by the requirement that the detector be sensitive to minimum ionizing particles and have a reasonable response to gamma rays as well as the basic sensitivity to protons.

The basic requirement on the readout is maximum readable dynamic range and resolution consistent with the size requirements. Because of the wide range of radiation conditions anticipated, readable dose should extend from a few millirads to as much as 500 rads. A range of 5 millirads to 500 rads represents an over-all range of $10^5:1$. This might in principle be compressed into a logarithmic scale as is commonly done in survey meters of various types. The limitation of a logarithmic scale is the inability to read small dose changes super-imposed on top of a relatively large dose, and thus

indications of rate are rather difficult to obtain. A multi-scale instrument having fine, medium and coarse indicators would permit a linear scale instrument to have sufficient dynamic range. If one considers an instrument with a circular scale of approximately 1" diameter or 75mm circumference, then 100 divisions on such a scale would represent a distance of 3/4mm per division. This is easily readable at normal viewing distances. Three scales then, each bearing a 100:1 relationship to each other would permit a potential rangeability of $10^6:1$ or an order of magnitude greater than that required by the extreme dynamic range. Such an indicator was created through the modification of a conventional watch face. This three scale instrument has proven exceptionally readable in a wide variety of environments and represents a format reasonably familiar to everyone. Its most severe disadvantage lies in the ratios of 60, 60 and 12 which corresponds to our non-decimal divisions of the day into seconds, minutes and hours. To bring this face into keeping with a decimal sub-division, scale factors of 50, 50 and 10 are adopted. While this provides a rangeability of only 25,000:1 a loss of resolution by requiring closer interpolation between divisions on the least significant scale is a small price to pay for the immediate and obvious readability of the most significant scale. This compromise was considered most appropriate since it places the greatest readability in that portion of the scale where the potential hazard exists. A watch mechanism itself represents perhaps the most compact wide range indicating instrument which is presently available in electromechanical technology. In particular, the tuning fork driven watch movement manufactured by the Bulova Watch Company for its Accutron wrist watches seemed particularly suitable especially in view of its previous application in satellites for timing and control.

The electronic system for transforming the impulses of charge collected in the detector into the deflection of the Accutron watch movement, is necessarily of some complexity. In brief, it consists of a charge sensitive preamplifier producing pulses proportional to the charge associated with the individual interactions in the detector, a multi-scale amplifier capable of bringing these pulses up to a level suitable for total charge integration, a threshold integrator converting these pulses into a current proportional to dose rate, an electrochemical cell capable of integrating this current

in the form of a total amount of material deposited in the cell, and a readout circuit capable of translating this integrated dose into a time interval to be measured by the output indicator. Power is provided from silver oxide primary cells providing in excess of 500 hours of over-all operation. A small DC-DC converter provides bias for the detector. In order to meet the packaging requirements two different construction techniques have been employed. Preamplifier-amplifier is a thin film hybrid unit occupying slightly more than 1/2 cu.in for a 12 transistor amplifier. the remaining circuitry being built with subminiature components on an etched circuit board which serves as a supporting chassis for the complete assembly. The power supply is housed in a separate plug-in modular configuration to permit ease of interchange of the primary power source and possible future modification of the dosimeter for operation off suit or spacecraft power.

5. DETAILED SYSTEM DESIGN

5.1 Detector

The silicon junction nuclear particle detector can be regarded as an ionization chamber in which one electronic charge is collected for every 3.5 electron volts of energy dissipated in the active volume of the device. The charge then collected is given by E , the charge on the electron divided by 3.5 coulombs/eV. Since there are E joules eV the electronic charge cancels out and $1/3.5$ coulombs/joule is collected. For a detector mass of one gram this would represent $1/3.5 \times 10^{-5}$ coulombs collected/rad or 10^{-8} coulombs/millirad. Significant dose rates range down to the order of 1 to 2 millirads/hour thus the collected current of these dose rates would be less than 10^{-11} amperes. Since at normal temperatures, thermally generated currents in the silicon detector are several orders of magnitude larger, it is clearly impractical to attempt to collect and measure the charge collected in the detector by simply measuring the integral of the DC current flowing, as is done in gas ionization chambers where leakage currents can be reduced to the 10^{-15} ampere range. It is then necessary to be able to observe the pulse of charge collected from each ionizing event in the detector which, because it is a discrete pulse can be amplified by conventional nuclear pulse amplification techniques. Under these conditions, the thermally generated DC leakage current can be ignored since it flows more or less as a continuous current and can be isolated from the system by means of a capacitor. The choice of an optimum detector configuration is based on a compromise between a number of considerations. Silicon detectors can be fabricated with the mass of the sensitive region of the detector ranging from 1 milligram to the order of a few grams. From the point of view of isotropic response a detector having a spherical sensitive volume is clearly the most desirable. While spheres have been fabricated, the reliability and reproducibility of such devices is in serious question. The response of a cube, which represents the simplest and reliable configuration for the detector, is very nearly equivalent to that of the sphere. The mass per unit area presented by the detector from various aspects differs less than 10% from an ideal sphere. From the point

low of maintaining a nearly ideal tissue response, the detector should be as small as possible since, when embedded in a mass of tissue equivalent material, the smaller the detector mass the less the perturbation of the population of secondary electrons produced in the tissue equivalent material. However, the available pulse heights vary inversely with the detector dimensions. A limit exists on the minimum pulse height which can be detected, imposed by the noise of the associated preamplifier. As a practical matter this limit is of the order of 50 keV for transistorized amplifiers operating over a wide temperature range. For this reason, it is desirable that all pulse heights of interest be large compared with this number. A minimum ionizing particle loses of the order of 350 keV per millimeter of silicon. This would then set the appropriate detector dimensions of the order of 1-2mm. Considerations of sensitivity at low rates dictate the use of the larger of these two figures and a detector of 2mm on edge has been adopted. The presence of this amount of atomic number 28 material in the tissue equivalent mass, tends to provide excess response for low energy secondaries since they will be completely stopped in the detector. On the other hand, the necessity of imposing a cut-off on energy due to amplifier noise, tends to result in a deficient response in this region. The preservation of response to gamma rays over a wide energy range is achieved by the use of a detector of this thickness. The response to fast protons is almost independent of the choice of detector thickness provided the detector is thin compared with the range of the protons of interest. This energy range is determined by consideration of the depth at which ionizing radiation is most likely to produce the greatest damage. As this is the order of several centimeters the most interesting range of proton energy is of the order of 100-200 MeV. These particles will deposit their maximum amount of energy at depths of several centimeters while protons of lesser energy will be stopped in the superficial layers of skin and muscle. The more energetic protons will completely penetrate the body and represent an LET only slightly greater than electron. A 2mm detector is clearly thin compared with the range of these particles and therefore should reflect the dose quite accurately in the range of interest. The largest available pulse height from the detector will be approximately 20 MeV corresponding to the energy particle

which is just stopped in 2mm of silicon. Minimum ionizing particles deposit approximately 0.7 MeV. Gamma rays will produce a spectrum of pulse heights corresponding to the typical Compton distribution from zero up to the Compton edge. For energetic gamma rays this distribution is rather flat with energy and the photo and pair production contribution is almost negligible. At energies of 100 keV and lower, the gamma processes tend to be more and more concentrated in photo processes resulting in electrons having the full gamma ray energy. At approximately 50 keV the energy absorbed/unit mass of aluminum, which is very similar to silicon is more than double that absorbed by tissue. At 100 keV these are nearly the same. However, as a result of the presence of a 50 keV threshold imposed by the electronics, no energy deposition by Compton processes at 50 keV will be observed and a deficit of approximately 1/2 at 100 keV will exist. Thus in first order the apparent dose lost due to the ignoring of Compton processes by the energy threshold tends to be compensated for by the excess photo processes in the higher atomic number silicon as opposed to tissue. A detector is surrounded by approximately 2mm of tissue equivalent material in order that equilibrium exist for the secondary electrons generated from gamma rays up to 1 MeV. This is a compromise directed toward avoiding excess material which would increase the threshold for good proton dose measurement. It is unfortunate that the achievement of good gamma dosimetry and good proton dosimetry is somewhat antagonistic in a single instrument. However, the 2mm tissue wall appears to be a reasonable compromise. The tissue equivalent material selected is a silicone rubber in which the silicon detector is known to be stable. The average Z is slightly higher than the equivalent average Z of tissue since it is somewhat deficient in oxygen and contains an appreciable silicon content. However, this tends to be compensated for by slight excess of hydrogen. The detector is then canned in a TO-5 transistor can contributing somewhat to the proton energy threshold by virtue of approximately 10 mils of stainless steel. The canning of the detector was felt to be essential to the assurance of long term reliability and stability of the detector.

5.2 Amplifier

As has been discussed, the system performance is largely dependent upon the noise level and dynamic range of the amplifier associated with

the detector. If a threshold is to be placed at 50 keV, the noise level of the amplifier must be sufficiently low that the probability of exceeding this threshold is vanishingly small, otherwise integration over long periods of time of the noise pulses which exceed the threshold will represent the accumulation of a false dose. In order to reduce the probability of a noise pulse crossing this threshold, it is necessary that the RMS noise be less than 1/6th of the threshold or less than 8.33 keV. Multiplying by 2.35 to convert to FWHM one gets a permissible amplifier noise of 19.6 keV (FWHM). The minimum noise is generally achieved when the amplifier contribution and detector contribution are approximately equal. This condition comes about by the selection of a shaping time constant in the amplifier which equalizes the shot noise contribution of the amplifier with the leakage current noise of the detector. Since these noises add incoherently, the permissible amplifier noise is 19.6 keV divided by the square root of 2 or approximately 14 keV. As this represents most of the state of the art for low power transistorized amplifiers, extreme care in the design of the amplifier and selection of components must be used to insure meeting this figure. The conventional charge sensitive amplifier configuration employing an operational integrator as the input element was chosen, as displaying very nearly the optimum noise and calibration stability of all possible amplifier types. Drawing C1502E1554-65 is a schematic diagram of the amplifier. The detector is connected between terminals D and E and supplied with positive bias through the load resistor R_4 and the decoupling network R_3-C_1 . As noise and ripple on the detector bias supply contribute directly to the noise of the amplifier, this decoupling is essential to remove any residual noise from the detector bias supply. Negative signals from the detector are coupled through C_2 to the base of the input transistor Q_1 . In order to minimize Miller effect in Q_1 its collector load is extremely low, being the input of a grounded base transistor stage Q_2 . This is a familiar cascode connection almost universally employed in low noise nuclear pulse amplifiers. While the voltage gain of Q_1 is less than unity, its current gain is equal to the beta of the transistor. The transistor is selected to have a beta in excess of 100 at approximately 10 microamperes the operating current of Q_1 and Q_2 . The grounded base stage Q_2 supplies

the voltage gain for the operational integrator; its output is connected to an emitter follower Q_3 in order to provide an impedance match to the load and the feedback path. R_{10} the collector load for Q_2 is bootstrapped by means of feedback through C_6 from the emitter of Q_3 . This bootstrap connection is necessary to maximize the open loop gain of the operational integrator while still preserving the appropriate stability conditions. Feedback for the operational integrator is through C_6 which determines the sensitivity of the preamplifier. This sensitivity can be expressed as

$$V_0 = Q_i / C_f$$

where V_0 is the output voltage from the emitter of Q_3 , Q_i the input charge from the detector and C_f the feedback capacitor C_6 equal to 50p. The input charge is most conveniently expressed in terms of equivalent energy deposited in the detector.

$$Q_i = E_i / 3.5 \times e$$

where E_i is the input energy, e is the electronic charge, and 3.5 arises from the energy in electron volts necessary to produce one hole-electron pair. Inserting numbers, then

$$Q_i = E_i \times 5 \times 10^{-14} \text{ coulombs/MeV}$$

Inserting this value for Q_i in the previous equation

$$V_0 = E_i \times 10^{-2}$$

or

$$V_0 / E_i = 10 \text{ millivolts/MeV}$$

A true operational integrator would be severely limited at high count rates since the output would continue to grow with successive input pulses without limit. For this reason, departure from an ideal integrator must be introduced by by-passing the feedback capacitor with a resistor. This time constant is usually made of the order of 100 micro-second in order to avoid introducing excess undershoot when successive differentiation takes place. The required resistor would be of the order of 20 meg ohms. The use of such a resistor across C_6 is impractical

for two reasons. First a generation of such high value resistors in thin film hybrid circuitry is exceedingly difficult since the resistors are formed by evaporation of thin metal film. In addition, since the base bias for Q_1 is established through this resistor, instability of the bias point with temperature would be the consequence of changing base current through such a large value of resistor. For this reason, a feedback network consisting of R_{11A} and R_5 is used to effectively reduce the magnitude of the feedback resistor to a more practical size. R_{11A} and R_5 form a 7:1 attenuator between the emitter of Q_3 and the return point for R_{11} the base resistor. Thus, from the feedback time constant point of view, the 1 meg ohm resistor in the base return circuit is effectively seven times as great. While this is admittedly a compromise from the 20 meg ohm most usually employed, the resulting 35 microsecond time constant is adequate to assure proper operation in subsequent parts of the system. The DC feedback provided by this path serves to stabilize the operating point of the amplifier in the presence of changing $B+$ voltage and varying temperature. Other versions of this amplifier built for other applications have shown good stability from a $B+$ of 6 volts to 18 volts over temperature ranges from -40°C to $+65^{\circ}\text{C}$.

The rapidly rising slow decaying step signals from the operational integrator preamplifier must then be processed to provide optimum noise response for the system. This is generally shown to require an integrating and differentiating time constant approximately equal. Experimentally values of near 1 microsecond were found to represent the best noise performance consistent with good performance at high counting rates. The shaping amplifier which follows the preamplifier uses the same circuit as the subsequent voltage amplifiers with the exception of the inclusion of feedback integration and interstage differentiation. These three stages will then be discussed at the same time. The requirements for voltage amplifier stages arise from the extremely wide dynamic range of pulses which must be processed in the dosimetry system. As we have seen, pulses ranging from 50 keV threshold to 20 MeV pulses from protons, must be processed with good linearity. This represents a voltage range of .5mv to 200mv at the output of the preamplifier. In order to impose a reliable threshold later in the system, the minimum signal of 0.5mv must

be amplified approximately 1000 times to of the order of 500mv in order to use the $\approx 500\text{mv}$ energy gap of a silicon transistor as a threshold device. If linearity is to be preserved, this would imply a dynamic range corresponding to 200 volts for the largest signals. Clearly in a low power transistorized amplifier, the achievement of such a high voltage output is not practical. For this reason, a multi-scale amplifier must be used. By multi-scale amplifier is meant an amplifier chain in which signals corresponding to large inputs are taken off early in the chain for subsequent processing and are permitted to saturate the stages later in the chain whereas low level signals are amplified by the later stages to provide linear outputs. Three such outputs are used, the highest level going from 5 MeV to 20 MeV, the next from 0.5 MeV to 5 MeV and the last from 50 keV to 0.5 MeV in which these limits represent the 500mv threshold and a 5 volt saturation level respectively. The requirement on the amplifier stages is that they have an accurately controlled gain of 10 with linearity up to 5 volts and graceful overload characteristics. In addition of course, power consumption must be kept to an absolute minimum. In order that the amplifier be non-inverting a two stage amplifier loop is indicated. The large available output swing of up to 90% of the B_+ voltage and low power consumption is obtained by the use of complementary stages in which the quiescent current is made as low as possible consistent with maintaining good gain bandwidth product for the transistors used. In order to obtain the necessary stability over-all feedback is used. The first stage is a difference amplifier using two n-p-n silicon planar transistors of the 2N930 general type. The difference amplifier compares the input signal with a portion of the output signal and supplies the amplified difference signal direct to the base of the p-n-p output transistor. Referring typically to the second stage, feedback to determine the gain of the amplifier stage is determined by R_{27} and R_{28} 10K and 90K ohms respectively. DC stability is insured by R_{26} and C_{13} which provide very high feedback at DC in order to stabilize the operating point in the presence of changing temperature and changing B_+ voltage. The operating point of Q_7 is determined by a base divider consisting of R_{22} and R_{23} which fix the base voltage at $1/2 B_+$ voltage. DC feedback will then fix

the base of Q_8 within a few millivolts of this point. The divider consisting of R_{26} , R_{27} , R_{28} and R_{29} determines the operating point of the output transistor since the voltage at the collector of Q_9 will assume a value which makes the base of Q_8 assume the same voltage as the base of Q_7 . In order for the base of Q_8 to be 3 volts, the current through the series combination of R_{26} and R_{27} will be 3 volts divided by 140K or approximately 22 microamperes. This 22 microamperes flowing through R_{28} produces a drop of 2 volts. The collector of Q_9 then operates at approximately 1 volt. In the actual case this steady state operating voltage is somewhat lower due to the base current drawn by Q_8 . The excursion of the output signal is limited by saturation of Q_9 . Since the saturation voltage of Q_9 is of the order of 0.2 volts, an output voltage swing of 5 volts is obtained with a 6 volt supply. The stability of the saturation level is assured by the DC feedback path described earlier. Under saturation the collector of Q_7 is connected back to the positive supply. Q_7 then effectively becomes an emitter follower due to the common emitter resistor R_{24} . Thus the high input impedance is maintained even in the presence of deep saturation so no excessive charging of C_{12} the coupling capacitor is experienced. This permits the circuit to recover within the length of the pulse from extreme overloads. The shaping amplifier consisting of Q_4 , Q_5 and Q_6 is similar with the exception of the inclusion of C_9 to limit the high frequency response to an optimum value and the increased gain of the stage due to R_{18A} and R_{18} in parallel in order to compensate for the pulse height losses accompanying pulse shaping. To provide sufficient open loop gain the common emitter resistor value is halved at the expense of additional stand-by power consumption. Differentiation is accomplished by C_{10} and R_{21} to provide a 1 microsecond decay constant. As a result of the differentiation the available pulse height excursion at terminal F is limited to 3 volts instead of 5 volts, resulting in saturation level of 30 MeV at the input. Since, as we have seen, the largest pulse possible in the detector is of the order of 20 MeV adequate dynamic range exists to avoid saturation at high levels. Since a gain of ten is obtained in each of the three amplifier stages, a gain of 10^3 from the preamplifier permits raising 50 keV signals to 500 millivolts at output H.

5.3 Anticipated Counting Rates

It is important to express the dose-rate in terms of counting rates of various size pulses in order to determine the effects of pulse pile up and overload. The mass of a 2mm cubical detector is given by $V\rho$, the volume V is $8 \times 10^{-3} \text{ cm}^3$ and the density of the crystal 2.33 grams/cm^3 . This gives a mass of $18.6 \times 10^{-3} \text{ grams}$. Since one rad deposits 100 ergs/gram, one rad would deposit in the detector $100 \times 18.6 \times 10^{-3}$ or 1.86 ergs. This is 1.86×10^{-7} joules or since there are 1.6×10^{-19} joules/eV there will be deposited approximately 1.2×10^{12} eV/rad or $1.2 \times 10^6 \text{ MeV/rad}$. In a radiation field of 1 rad/hour this would imply 330 counts/sec for 1 MeV pulses and about 500 counts/second for minimum ionizing pulses. As the amplifier can accommodate pulse rates up to about 50,000/second, there should be no difficulty in accommodating any conceivable radiation dose-rate which might be encountered in a space situation. If the $1.2 \times 10^6 \text{ MeV/rad}$ has the basic detector response multiplied by the sensitivity of the amplifier in volts/MeV, then the result is a figure having the dimensions of volts/rad and is numerically equal to 1.2×10^7 for the H or highest gain output, i.e. the product of the number of events and the pulse height for an integrated dose of 1 rad is equal to this figure.

5.4 Pulse Integrator

The outputs from the amplifier must be integrated to provide total dose information. Since the rate of accumulation of dose varies over very wide limits, rather exacting demands are imposed on the integration circuitry. Conventional operational integrators are limited by leakage current to integrating times of a few minutes. Since significant doses may be accumulated over periods of hours, such integrators are obviously not suitable. Electrochemical integrators have been investigated as a means of providing drift free integration over periods ranging from seconds to hours. Among the devices investigated are the Memister which consists of an electrochemical cell in which metal is plated from an electrolyte on to a resistive substrate in order to provide a conductance proportional to integrated plating current, the Solion cell which integrates by electrochemical conversion of iodide iron to iodine and subsequent diffusion of free iodine through a semipermeable membrane, various

types of coulometers involving visual readout of a column of plated material, and the Bissett Berman E-cell. The first two were basically found unsuitable as a result of the tendency to show zero drift in the absence of a plating current. The visual readout coulometers tend to lack sensitivity and scale readability. The Bissett-Berman E-cell has shown the greatest promise and was adopted. Briefly, this cell consists of two carefully prepared noble metal electrodes immersed in an electrolyte containing an excess of silver ions. A measured amount of silver is plated from an external electrode on to one of the electrodes and the cell sealed by crimping of a platinum seal-off tube. Subsequent adjustment of the amount of free silver in the cell can be accomplished by plating some of the originally deposited material on to the platinum seal-off tube. Integration takes place during the passage of a current from zero to 10 microampere through the cell with the silver coated reservoir being the anode. In accordance with Faraday's principle one gram equivalent of silver is transferred for every 96,500 coulombs passed through the cell. This process continues either until the silver reservoir is completely depleted, detected by a rise of potential across the cell, or the cell is read out. Readout consists of reversing the plating current and measuring total charge necessary to return all the silver back to the reservoir detected again by an increase in voltage drop across the cell. Since silver can transfer only with the passage of current the cell is stable as long as the current passing through is zero. The plated material can be permitted to remain indefinitely on either electrode and the cell restored to the original state by plating it to the reservoir. While definite temperature limitations are imposed by the freezing of the electrolyte at approximately -30°C , it appears to offer a suitable integration means for the dose recorded by the system. The pulses from the amplifier cannot be integrated directly by the E-cell for two reasons. First, the pulses necessarily are bi-polar i.e. contain no DC component since they are capacitively coupled both within the amplifier and at the output. Secondly, any attempt to integrate the pulses directly would result in integrating noise which, though small in amplitude, is present continuously and therefore can result in the accumulation of appreciable apparent dose. The latter problem is dealt with by means of three emitter followers which are biased to present a

threshold of 500 millivolts to the incoming signal. This corresponds to the energy gap of a zero biased silicon transistor. In drawing B1503E1554-65 these are Q_1 , Q_2 and Q_3 . Signals to any of these three inputs must exceed 500 millivolts before any output appears at their emitters. In order to convert the bi-polar input pulse to a unidirectional current, a non-linear element must be introduced. However, such non-linear elements must not distort the basic linearity of the system, i.e. in spite of the presence of these elements, the integrated charge should be equal to the pulse height, pulse rate integral of the input. To prevent the non-linear elements, in this case diodes D_2 and D_3 from affecting the linearity of the system, the E-cell, its bypassed capacitor C_7 and diodes D_2 and D_3 are placed in the feedback loop of an operational integrator composed of Q_5 and Q_6 . Q_6 serves as the integrator having the E-cell and its associated components connected from collector to base, and Q_5 serves as a switch to ensure zero output from the integrator in the absence of a pulse above threshold. In order to understand the action of the integrator, consider a pulse from the amplifier applied to the base of Q_3 . If this pulse is in excess of 500 millivolts, Q_3 conducts. The base emitter junction of Q_4 is in its collector circuit and Q_4 , which has been normally bypassed off, turns on, clamping the base of Q_5 to $B+$. Previously, R_9 turned on Q_5 clamping the collector of Q_6 to approximately 0.5 volt below $B+$ as determined by D_1 . The low impedance of the saturated transistor Q_5 prevents any small signals present at the collector of Q_6 from overcoming the diode gaps of D_2 and D_3 and hence causing spurious integration of charge in the E-cell. However, as Q_5 is cut off by the saturating of Q_4 , the collector of Q_6 is free to fall from its previous value. The charging current of C_3 flows into the base of Q_6 . As its collector falls, the charge flowing into C_3 from the emitter of Q_3 , is supplied by the feedback path through D_2 depositing a charge on C_6 proportional to the charge on C_3 . At the conclusion of the pulse, Q_5 conducts once more transferring this charge through D_3 to the E-cell. Higher level signals overcome the threshold of either Q_2 or Q_1 the total charge being summed into the base of Q_6 through capacitors determined by the desired scale factor. The amount of charge deposited on the E-cell is simply equal to the summing capacitor C_3 , C_2 or C_1 times the pulse

voltage. Considering now C_3 the charge delivered will be 50 pc/volt. Multiplying this by the previous sensitivity figure of 1.2×10^7 volts/rad we get an integrated charge of $1.2 \times 10^7 \times 50 \times 10^{-12}$ or 600 microcoulombs/rad. At a dose rate of 1 rad/hour, this results in a current of 600 microcoulombs divided by 3600 seconds or 1/6th of a microampere for a 1 rad/hr dose rate. Since the E-cell can tolerate 60 times this dose rate, the E-cell and integrator impose a limitation of 1 rad/minute for the incident dose rate. The same scale factor holds for higher energy signals capable of overcoming the threshold of Q_2 or Q_1 . Since each volt at this point represents either ten or one hundred times the incident dose rate, the capacitors C_1 and C_2 are made ten and one hundred times larger than C_3 respectively. The 500 millivolt threshold introduces no appreciable non-linearity in the response for the following reason: If a signal has sufficient height to exceed the threshold of Q_1 , the 500 millivolt which it loses across the threshold gap is just compensated by the saturating signal appearing at the base of Q_2 but coupled into the integrator by 1/10th the capacitance. The same is true of the 500 millivolt gap at Q_2 being compensated by the corresponding saturation signal at the base of Q_3 . The 500 millivolt gap at the base of Q_3 is compensated for by a step at the collector of Q_4 , capacitor C_4 adds in the appropriate charge to make up for that lost.

The readout from the electrochemical cell is accomplished by means of a control flip-flop consisting of Q_7 and Q_9 . Readout is accomplished by reversing the directional current flow through the E-cell and measuring the time required for a constant current to reverse plate the silver initially transferred during dose accumulation. Initially, assume Q_9 is conducting. The collector of Q_9 is then clamped within 0.1 volt of its emitter. Q_7 is then cut off since its base is returned to its emitter and diode D_4 is reverse biased. The E-cell accumulates in a normal way. The operating point for the base of Q_6 is determined by the potential of the saturated collector of Q_9 . Readout occurs if either one of two conditions is fulfilled. If the E-cell is completely plated across, the voltage across the E-cell begins to rise due to the integrator attempting to push additional charge through the cell when there is no more

platable silver available. This causes a rise in the base of Q_7 until it conducts cutting off Q_{10} and Q_9 through the usual flip-flop action. Cutting off Q_{10} causes the output indicator to run, as will be seen later. When Q_9 is cut off, its collector current then flows through the E-cell in the opposite sense to the original plating current, returning to the common through the base of Q_7 . This keeps Q_7 conducting as long as reverse plating is taking place. Alternatively, the readout process may take place on demand by pushing the readout switch which momentarily cuts off Q_{10} . If platable material is available on the E-cell, the flip-flop will remain in this state until this material is reverse plated. As reverse plating nears its end point, the collector of Q_9 begins to rise since the E-cell can no longer maintain a low voltage drop without platable material being available. This rise in potential raises D_5 and D_6 into conduction causing the silicon control switch Q_8 to become conducting and clamping the collector of Q_9 to its emitter. This cuts off Q_7 and the original state is maintained. Since reverse plating takes place with 10 microamperes, the 600 microcuries/rad results in a 60 second readout cycle/rad. This corresponds to one revolution of the second hand on the readout timer establishing the scale factor of 1 rad/revolution for the second hand.

5.5 Readout Circuit

As has been previously discussed, the Accutron watch movement is used as a basis of scaling the time necessary to back plate the E-cell for a given charge. This is a ruggedized version of the tuning fork driven wrist watch in common use. Several requirements have had to be met in order to make this device useful for reading out the dosimeter. First, the gear ratios have been altered such that a consistent ratio between scales is established. The second hand represents 1 rad/revolution. Since the watch face is divided into ten major divisions each of these corresponds to 100 mr and in turn each of the major divisions into five minor divisions corresponding to 20 mr each. Since the eye can easily resolve half of one of these divisions, 10 mr represents the resolution of the readout system. The minute hand makes one revolution for every 50 revolutions of the second hand, thus it represents 50R/revolution or 5R for each major division and 1R for minor division. The hour hand makes

one revolution for each ten revolutions of the minute hand, giving a full scale unambiguous output to 500R. The Accutron movement presents some difficulty in being used in the intermittent mode. As normally used it runs continuously and is somewhat sluggish in starting. In fact, in general, it will not start by itself but must be given a sharp tap to set the fork initially in motion. While this is useful in a watch in order to provide a precise setting feature, it is clearly a source of difficulty in the present application. In addition, the large amount of stored energy in the tuning fork, tends to cause the watch to continue to advance after power is removed from the fork. While these two effects, that of a sluggish start and coasting after stop, tend to cancel, unfortunately, they are both temperature sensitive and therefore are to be minimized. The circuit involving Q_{11} , Q_{12} and Q_{13} is directed toward that end. Q_{13} is the basic oscillator to sustain tuning fork oscillations. The tuning fork drive winding is connected in its collector feedback winding supplying base drive. R_{21} and C_{13} maintain the appropriate base bias. C_{11} is required to suppress high frequency oscillation modes which result from incidental electromagnetic coupling between the drive and feedback windings and a frequency far removed from the fork oscillation frequency. In order to prevent coasting, or for that matter any motion of the watch after power is removed, Q_{11} is kept saturated across the drive winding. This acts as a dynamic brake reflecting a very large damping factor into the fork through the drive winding. Q_{12} supplies the basic drive power as a series switch. It is normally biased off when Q_{11} is conducting. The watch is started when Q_{10} is cut off. This cuts off Q_{11} removing the damping from the drive winding and permits R_{18} to saturate Q_{12} , effectively connecting the drive winding to B+. C_{12} is normally charged to approximately 2 volts by a small amount of leakage current which is fed to the circuit through R_{19} . When Q_{12} is saturated then, initially four volts or approximately twice the operating voltage is imposed across the drive circuit for a period of a few milliseconds. As C_{12} charges to its equilibrium value, the voltage drop across the drive circuit falls to its nominal value of 1.5 volts. This high initial transient voltage across the drive circuit causes rapid starting even in the absence of an initial impulse. The watch runs until Q_{10} once again saturates, turning on Q_{11} and off Q_{12} and returning the circuit to

its quiescent state. While the circuitry involved in integrator and drive circuits may appear quite complex, considerable effort has been devoted to reducing it to simplest terms consistent with achieving the required operation. Attempts have been made to minimize bulky components with the result that the entire circuit occupies less than 1 cu.in.

5.6 DC to DC Converter

In order to provide approximately 150 volts bias for the detector, a DC to DC converter is required. With a view of maximum simplicity, a single ended blocking oscillator type of converter was used. Drawing A1502E1554-65 shows the circuit adopted, a subminiature audio transformer is used to provide a step-up of approximately 22:1. The operating frequency is kept below 1 kilocycle to conserve power, as determined by the .005 microfarad capacitor and 750K resistor used in the base of the feedback circuit. A simple half way rectifier is used followed by a π section RC filter to remove any residual ripple. Power consumption is approximately 60 microamperes at 6 volts for 1 microampere output at 150 volt giving an efficiency considerably better than 30%. To provide greater flexibility in power supply and to minimize possible interference between the DC to DC converter and the low level circuitry, the DC to DC converter is contained in the power module which is separable from the mainbody of the instrument.

5.7 Primary Power Source

A number of different primary power sources were investigated with a view of providing the greatest operational flexibility consistent with the duration of the mission. Rechargeable batteries of a nickel cadmium or silver cadmium type were considered from the point of view of convenience, particularly during calibration and ground handling. Since these are rechargeable during periods of idleness the instrument is always in a state of readiness for use. Unfortunately, the amount of space required for rechargeable batteries sufficient to provide power between chargings for one complete mission, is greater than the space which could be allotted. For this reason, the primary battery of the silver oxide-zinc type was used.

This battery type originally developed for use in compact hearing aids, electric watches and similar applications represents the most compact source of energy available capable of working over reasonable temperature range. The individual cells are contained in a detachable power module along with the DC to DC converter capable of being changed in flight if necessary. This module was originally designed to be made from plastic to minimize weight and provide electrical insulation. However, structural considerations forced a change to anodized aluminum.

6. MECHANICAL DESIGN

The basic mechanical design of the unit is shown in drawing C1503M1554-65. As is obvious considerable crowding is required to fit in all the necessary components. The package is basically divided into two sections, the dosimeter and the power supply module. The power supply module is a plug-in assembly containing the DC to DC converter for bias and the silver oxide cells for basic power supply. By making this unit separable, the system is readily adapted to using other sources of power. Twelve Union Carbide Eveready type S76 silver oxide cells are used in three stacks of four each. These cell stacks are connected in parallel by a beryllium copper contact assembly in the bottom of the wells provided for the batteries, the ground being effected on the negative side of the batteries through a beryllium copper contact strip which closes the side of the compartment. The dosimeter itself consists of five major components, the detector assembly, the amplifier assembly, the demand readout switch and the modified Accutron watch, together with the circuit board assembly which supports all internal components except the watch movement and has built on it the threshold integrator and readout circuits. It is secured to the thin wall aluminum housing by means of four screws from the back side. Two additional screws support the amplifier assembly. The detector is provided with a socket to permit its being interchanged without damage to the detector assembly or other components. In order to fit into the available space, a special subminiature switch assembly was fabricated using a type A5-71/P3 microswitch and a push button assembly built into the case wall. The details of this are self-explanatory in the drawings. The watch movement itself is supported directly from the case by means of four mounting screws, into the front of the case. Removal and replacement of the entire assembly is accomplished through the removal of all screws permitting the flush mounted watch movement to drop down slightly below the surface of the housing. The circuit board and watch movement can now be removed by sliding out through the open end of the housing. Because of the small physical size and low mass of all the components employed, little difficulty is anticipated in surviving the Apollo shock and vibration requirements. The most vulnerable part of the instrument

is the thin aluminum housing itself. Since it is anticipated that this will be carried in a pocket in the space suit, most of the G load will be rather uniformly distributed over its outer surface and for this reason relatively thin housing reinforced by the rather massive power supply compartment should be able to withstand all stresses that might conceivably be applied to it. The power supply compartment is designed to be removable in flight should a change in mission profile require more battery life than is readily obtainable from the silver oxide cells. It is secured in place by two ball catch type fasteners which are capable of maintaining its position under rather severe loads. Space is available for a semi permanent fastener to augment this should it be required.

The push button presents some difficulty in arriving at an optimum design. In order to avoid the possibility of projecting items catching on the material of the space suit, a flush push button design was indicated. On the other hand, some difficulty may be experienced depressing flush push button with a heavily gloved hand. The method of assembly, however, lends itself to increasing the push button area almost indefinitely to include if necessary, the entire upper portion of the case. Only extensive trials with appropriately gloved hands will be able to decide this question. No attempt has been made to pressurize or hermetically seal the entire assembly. This would necessitate the use of a heavier walled housing with the consequent wasted space and weight. All components have been tested for operation in vacuum and no difficulty during pump down is anticipated. The watch movement itself is vented to prevent excessive stresses on the glass watch face during pump down. Because of the extremely low power dissipation in all parts of the system, no specific requirements for high temperature operation are required. The upper operating temperature is limited by the detector primarily to somewhere in the vicinity of 60°C. This represents the temperature at which lithium drift detectors begin to deteriorate quite rapidly due to undesired drift under bias. Considering that the instrument is in rather close thermal contact with the astronaut, there being essentially one thickness of suit between the dosimetry package and the inside air conditioned space, this is not an unreasonable temperature

limitation. Similarly, the low temperature limits dictated primarily by the freezing of the electrolyte in the electrochemical cell and the loss in capacity of the power source are not expected to be exceeded. Calibration will be hampered somewhat below 0°C as a result of the loss in performance at low power levels of the transistors employed in the amplifier and integrator. The surface finish has been chosen primarily for durability and handling in normal laboratory environments. It is probably desirable that a low emissivity surface be provided either in the form of stripping the anodized film and polishing the aluminum surface, or coating with a suitable low emissivity paint.

7. TEST AND CALIBRATION

Laboratory testing was performed on all components of the system in order to ensure conformity of the final components to their design specifications. Final calibration of the preamplifier, threshold integrator and readout circuitry was performed using a pulse generator applied to the test input of the preamplifier, the calibration of which was checked against the actual detector input with the aid of an unencapsulated detector and an α particle source. Because of the pressure of time for delivery, only a limited number of tests were performed on the completed instrument. These included response to Co^{60} gamma rays, and limited testing using the 40 MeV proton beam from the UCLA spiral ridge accelerator.

Temperature testing was performed on the preamplifier and threshold integrator to determine the effect, if any, of varying temperature on calibration stability. These tests were performed by introducing a fixed rate of a given amplitude pulse into the test input of the preamplifier and measuring the current integrated by the E-cell. Sensitivity from 0°C to 60°C varies less than $\pm 5\%$ for 6 V B+ power supply. Below 0°C , performance is rather sharply dependent on B+ voltage. For B+ voltage of 6-1/2 V, a loss in sensitivity of 10% is observed from 0°C to -30°C . At 5-1/2 V B+, this loss is 20%. Test runs at higher B+ voltage, namely 8, 9 and 10 volts, indicate that at these B+ voltages, temperature effects are essentially negligible to 0°C with a 5% decline in sensitivity at -30°C . This would call for a revision in the power supply voltage if extensive low temperature operation was anticipated.

The Accutron watch and readout system was temperature cycled over a similar range with a simulated input corresponding to approximately 2000 on-off-cycles. The timekeeping error of the Accutron is essentially negligible over the complete range, being in the neighborhood of a few hundredths per cent. However, a fixed error is associated with each start-stop cycle, ranging from approximately 1 millisecond at normal temperatures to as high as 10 milliseconds at -30°C . Since each second corresponds to 15 mr, this is a possible error of 0.15 mr per cycle.

If the system is cycled ten times per hour, this could represent a random rate error of approximately 1.5 mr per hour. If cycling of the readout system takes place less frequently, this error is correspondingly reduced.

Temperature effects on the detectors are measured principally in terms of variations in leakage current and noise with temperature. Leakage current for all detectors was nominally less than 1 microampere at room temperature and showed the characteristic doubling for each 11°C above room temperature. Because of the high output impedance of the DC to DC converter supplying bias to the detector, the voltage applied to the detector declines as leakage current tends to climb. This tends to keep the noise somewhat constant with a 5 to 10% decline in sensitivity at the higher temperatures. This effect appears to offset to some extent the temperature coefficient of the amplifier and threshold integrator in order to keep the overall response within $\pm 5\%$.

In the course of the temperature runs, substantial humidity testing was incidentally performed through the condensation of moisture on the circuits as a result of the rapidly changing temperature. On unencapsulated circuit boards, this led to excessive leakage into the E-cell with a result that apparent dose was accumulated even in the absence of any input. This effect was investigated and corrected by careful cleaning of the circuit board with deionized water and alcohol followed by coating with a conformal epoxy coating.

Because of the pressure of time, shock and vibration testing was not performed on the completed instrument. However, the most vulnerable element in the system, namely the Accutron watch movement, has been qualified for launch loads considerably in excess of those anticipated.

Absolute nuclear calibration can be carried out only by having available calibrated sources of radiation similar to those which are encountered in space. Two sources of calibrating fields were available within the time scale for delivery of the instruments. One, a 10 millicurie Co^{60} source capable of furnishing a reasonable uniform field

approximately 1 rad per hour and a 40 MeV proton beam from the UCLA spiral ridge accelerator. Calibrations using the Co^{60} source were approximately 20% lower than would be calculated from the source strength and distance. This can be accounted for by the low energy cut-off imposed by the threshold integrator, though the source calibration itself is only $\pm 10\%$. Calibration data from the 40 MeV protons was obtained by placing the detector in the scattered beam to avoid excess counting rates associated with the minimum direct beam which can be stably generated by the machine. Attempts to correlate the counting rate for protons in a monitor detector with the dose measured by the system produced quite erratic results. Upon investigation, it was found that the extremely rapid fall in the number of scattered protons per unit solid angle with angle made correlations between two detectors in apparently the same field quite difficult. For this reason, dose correlation between the calculated dose received by the monitor detector and the dose received by the instrument at a slightly different angle bear little relationship to each other. To attempt a more precise calculation, nuclear emulsions were placed over the sensitive area of the Apollo dosimeter system and the two were irradiated simultaneously. The nuclear emulsions are being scanned by the Health Physics personnel at UCLA, the results of which are not yet available for this report.

In order to provide the best possible calibration given the difficulties experienced, spectra were taken on the detector in a dummy case environment and channel by channel integration of the pulse height spectra obtained permitted calculation of the dose deposited in the detector by the 40 MeV protons. With the exception of a bump on the low energy side of the dE/dx peak obtained, this spectrum and the corresponding calculated dose corresponds quite well to that which would be delivered by 40 MeV protons degraded by the aluminum case. The readout resistor for the dosimeter was then adjusted such that a similar pulse distribution introduced by means of a pulse generator resulted in the appropriate readout in rads. Provision has been made for the shunting of this resistor in order to bring the scale factor into better coincidence with absorbed dose as better calibrated fields are available.

8. CONCLUSIONS AND RECOMMENDATIONS FOR ADDITIONAL WORK

From the amount of work which could be done within the time scale available, it would appear that the fundamental principle behind the Apollo dosimeter is sound and can yield reproducible and radiobiologically meaningful results. While the engineering design and mechanical packaging display some rough edges with regard to an instrument for actual flight use, the basic design and packaging concepts are sound. It has been shown that a dosimeter for the particle energy range and levels of interest for the Apollo mission can be fabricated within the envelope, weight and power restrictions associated with a self-contained personal dosimetry instrument. As the instrument design is verified and solidified, further reductions in size and weight and greater ruggedization are possible through the conversion of the remaining subminiature printed circuit board components to thin-film hybrid circuitry, as was done with the preamplifier and amplifier. As better semiconductors become available, performance over wider temperature ranges at reduced power can be expected. However, even at the present levels, adequate power for the mission duration is available.

The work to be done falls in the category of environmental testing and calibration verification in varied radiation fields. Such environmental testing includes verification of the shock and vibration performance, more definitive temperature and humidity information, and extensive life testing in the thermal vacuum environment simulating space. While the results of such testing will undoubtedly influence some of the detailed design and construction features of the instrument, it is not anticipated that any major revision of the concepts or techniques will have to be made as a result of such qualification. Verification of the radiation calibration requires a considerable amount of accelerator work with particular emphasis on obtaining homogeneous diffuse beams of particles in the energy range of interest in such a way that intercomparison of various dose measuring devices can be made. In considering possible calibration, it is necessary to determine what, if any, loading factors should be applied to the various LET of the interactions observed. Such

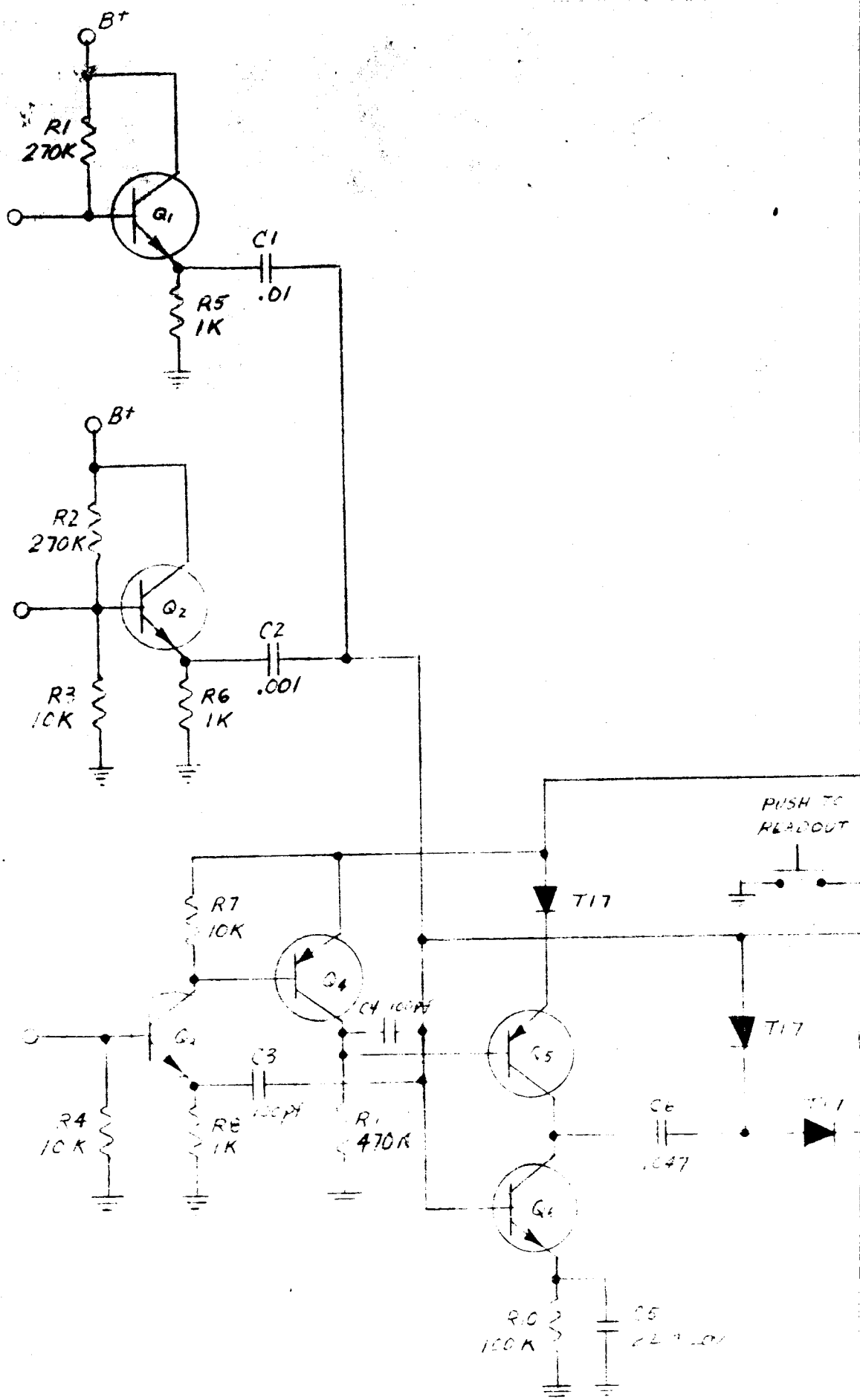
radiobiologically significant loading in accordance with LET is readily incorporated in the instrument due to its multi-scale integrator. However, until some general agreement on the part of radiation biologists can be arrived at, the uniform weighting which has been given to various LET levels will have to be relied on.



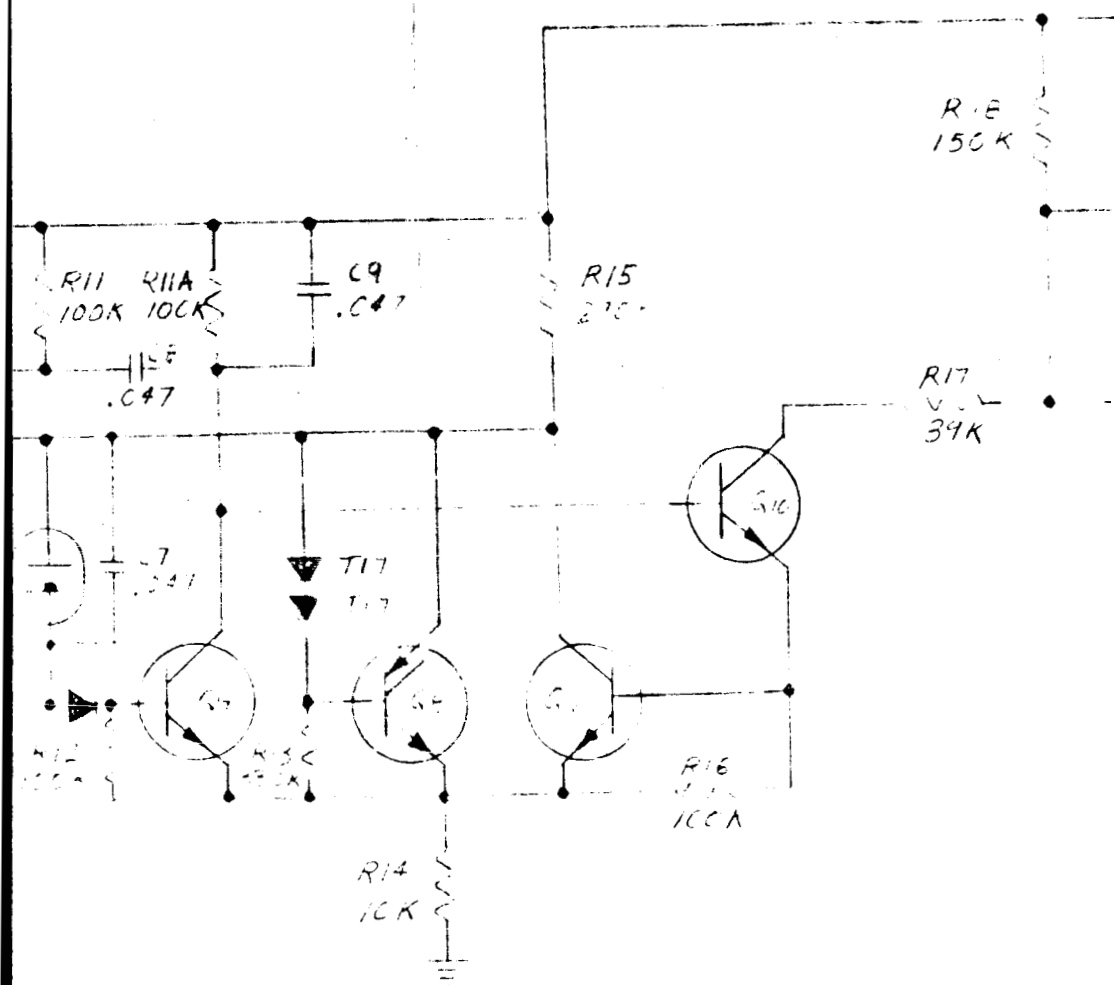
- A1502E1554-65**

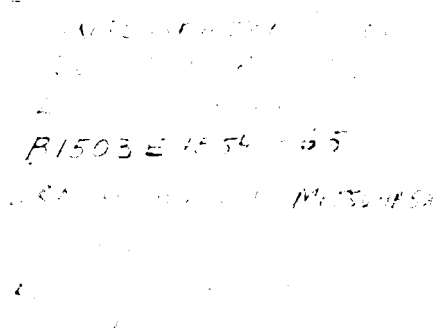
2024-10-27 09:07:00 AM

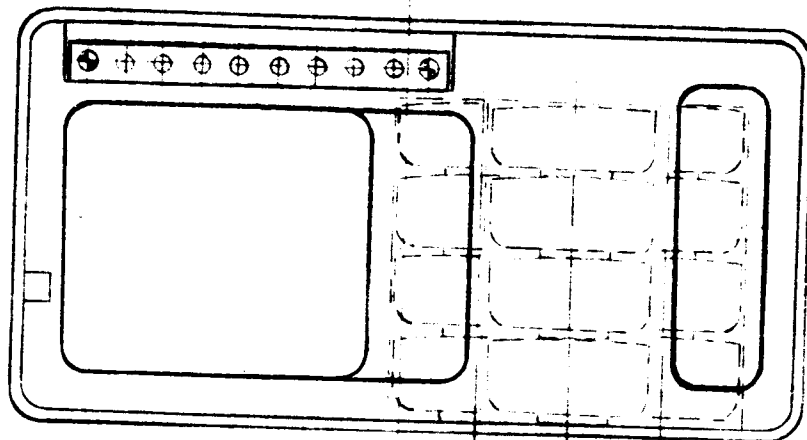
DC to DC CONVERTER FOR
PACMAN DCSIMPLE
ELECTRONICS



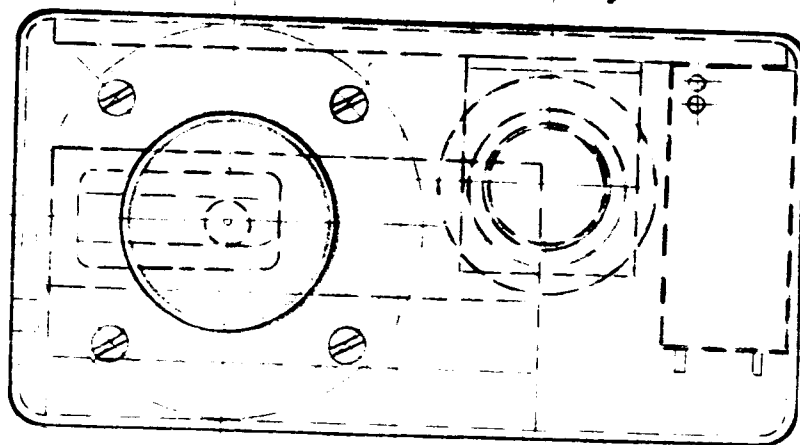
Q1, Q2, Q3, Q4, Q5, Q6, Q7, Q8, Q9, Q10, Q11, Q12, Q13, Q14, Q15, Q16, Q17, Q18, Q19, Q20, Q21, Q22, Q23, Q24, Q25, Q26, Q27, Q28, Q29, Q30, Q31, Q32, Q33, Q34, Q35, Q36, Q37, Q38, Q39, Q40, Q41, Q42, Q43, Q44, Q45, Q46, Q47, Q48, Q49, Q50, Q51, Q52, Q53, Q54, Q55, Q56, Q57, Q58, Q59, Q60, Q61, Q62, Q63, Q64, Q65, Q66, Q67, Q68, Q69, Q70, Q71, Q72, Q73, Q74, Q75, Q76, Q77, Q78, Q79, Q80, Q81, Q82, Q83, Q84, Q85, Q86, Q87, Q88, Q89, Q90, Q91, Q92, Q93, Q94, Q95, Q96, Q97, Q98, Q99, Q100, Q101, Q102, Q103, Q104, Q105, Q106, Q107, Q108, Q109, Q110, Q111, Q112, Q113, Q114, Q115, Q116, Q117, Q118, Q119, Q120, Q121, Q122, Q123, Q124, Q125, Q126, Q127, Q128, Q129, Q130, Q131, Q132, Q133, Q134, Q135, Q136, Q137, Q138, Q139, Q140, Q141, Q142, Q143, Q144, Q145, Q146, Q147, Q148, Q149, Q150, Q151, Q152, Q153, Q154, Q155, Q156, Q157, Q158, Q159, Q160, Q161, Q162, Q163, Q164, Q165, Q166, Q167, Q168, Q169, Q170, Q171, Q172, Q173, Q174, Q175, Q176, Q177, Q178, Q179, Q180, Q181, Q182, Q183, Q184, Q185, Q186, Q187, Q188, Q189, Q190, Q191, Q192, Q193, Q194, Q195, Q196, Q197, Q198, Q199, Q200, Q201, Q202, Q203, Q204, Q205, Q206, Q207, Q208, Q209, Q210, Q211, Q212, Q213, Q214, Q215, Q216, Q217, Q218, Q219, Q220, Q221, Q222, Q223, Q224, Q225, Q226, Q227, Q228, Q229, Q230, Q231, Q232, Q233, Q234, Q235, Q236, Q237, Q238, Q239, Q240, Q241, Q242, Q243, Q244, Q245, Q246, Q247, Q248, Q249, Q250, Q251, Q252, Q253, Q254, Q255, Q256, Q257, Q258, Q259, Q260, Q261, Q262, Q263, Q264, Q265, Q266, Q267, Q268, Q269, Q270, Q271, Q272, Q273, Q274, Q275, Q276, Q277, Q278, Q279, Q280, Q281, Q282, Q283, Q284, Q285, Q286, Q287, Q288, Q289, Q290, Q291, Q292, Q293, Q294, Q295, Q296, Q297, Q298, Q299, Q300, Q301, Q302, Q303, Q304, Q305, Q306, Q307, Q308, Q309, Q310, Q311, Q312, Q313, Q314, Q315, Q316, Q317, Q318, Q319, Q320, Q321, Q322, Q323, Q324, Q325, Q326, Q327, Q328, Q329, Q330, Q331, Q332, Q333, Q334, Q335, Q336, Q337, Q338, Q339, Q340, Q341, Q342, Q343, Q344, Q345, Q346, Q347, Q348, Q349, Q350, Q351, Q352, Q353, Q354, Q355, Q356, Q357, Q358, Q359, Q360, Q361, Q362, Q363, Q364, Q365, Q366, Q367, Q368, Q369, Q370, Q371, Q372, Q373, Q374, Q375, Q376, Q377, Q378, Q379, Q380, Q381, Q382, Q383, Q384, Q385, Q386, Q387, Q388, Q389, Q390, Q391, Q392, Q393, Q394, Q395, Q396, Q397, Q398, Q399, Q400, Q401, Q402, Q403, Q404, Q405, Q406, Q407, Q408, Q409, Q410, Q411, Q412, Q413, Q414, Q415, Q416, Q417, Q418, Q419, Q420, Q421, Q422, Q423, Q424, Q425, Q426, Q427, Q428, Q429, Q430, Q431, Q432, Q433, Q434, Q435, Q436, Q437, Q438, Q439, Q440, Q441, Q442, Q443, Q444, Q445, Q446, Q447, Q448, Q449, Q450, Q451, Q452, Q453, Q454, Q455, Q456, Q457, Q458, Q459, Q460, Q461, Q462, Q463, Q464, Q465, Q466, Q467, Q468, Q469, Q470, Q471, Q472, Q473, Q474, Q475, Q476, Q477, Q478, Q479, Q480, Q481, Q482, Q483, Q484, Q485, Q486, Q487, Q488, Q489, Q490, Q491, Q492, Q493, Q494, Q495, Q496, Q497, Q498, Q499, Q500, Q501, Q502, Q503, Q504, Q505, Q506, Q507, Q508, Q509, Q510, Q511, Q512, Q513, Q514, Q515, Q516, Q517, Q518, Q519, Q520, Q521, Q522, Q523, Q524, Q525, Q526, Q527, Q528, Q529, Q530, Q531, Q532, Q533, Q534, Q535, Q536, Q537, Q538, Q539, Q540, Q541, Q542, Q543, Q544, Q545, Q546, Q547, Q548, Q549, Q550, Q551, Q552, Q553, Q554, Q555, Q556, Q557, Q558, Q559, Q560, Q561, Q562, Q563, Q564, Q565, Q566, Q567, Q568, Q569, Q570, Q571, Q572, Q573, Q574, Q575, Q576, Q577, Q578, Q579, Q580, Q581, Q582, Q583, Q584, Q585, Q586, Q587, Q588, Q589, Q590, Q591, Q592, Q593, Q594, Q595, Q596, Q597, Q598, Q599, Q600, Q601, Q602, Q603, Q604, Q605, Q606, Q607, Q608, Q609, Q610, Q611, Q612, Q613, Q614, Q615, Q616, Q617, Q618, Q619, Q620, Q621, Q622, Q623, Q624, Q625, Q626, Q627, Q628, Q629, Q630, Q631, Q632, Q633, Q634, Q635, Q636, Q637, Q638, Q639, Q640, Q641, Q642, Q643, Q644, Q645, Q646, Q647, Q648, Q649, Q650, Q651, Q652, Q653, Q654, Q655, Q656, Q657, Q658, Q659, Q660, Q661, Q662, Q663, Q664, Q665, Q666, Q667, Q668, Q669, Q670, Q671, Q672, Q673, Q674, Q675, Q676, Q677, Q678, Q679, Q680, Q681, Q682, Q683, Q684, Q685, Q686, Q687, Q688, Q689, Q690, Q691, Q692, Q693, Q694, Q695, Q696, Q697, Q698, Q699, Q700, Q701, Q702, Q703, Q704, Q705, Q706, Q707, Q708, Q709, Q710, Q711, Q712, Q713, Q714, Q715, Q716, Q717, Q718, Q719, Q720, Q721, Q722, Q723, Q724, Q725, Q726, Q727, Q728, Q729, Q730, Q731, Q732, Q733, Q734, Q735, Q736, Q737, Q738, Q739, Q740, Q741, Q742, Q743, Q744, Q745, Q746, Q747, Q748, Q749, Q750, Q751, Q752, Q753, Q754, Q755, Q756, Q757, Q758, Q759, Q760, Q761, Q762, Q763, Q764, Q765, Q766, Q767, Q768, Q769, Q770, Q771, Q772, Q773, Q774, Q775, Q776, Q777, Q778, Q779, Q780, Q781, Q782, Q783, Q784, Q785, Q786, Q787, Q788, Q789, Q790, Q791, Q792, Q793, Q794, Q795, Q796, Q797, Q798, Q799, Q800, Q801, Q802, Q803, Q804, Q805, Q806, Q807, Q808, Q809, Q810, Q811, Q812, Q813, Q814, Q815, Q816, Q817, Q818, Q819, Q820, Q821, Q822, Q823, Q824, Q825, Q826, Q827, Q828, Q829, Q830, Q831, Q832, Q833, Q834, Q835, Q836, Q837, Q838, Q839, Q840, Q841, Q842, Q843, Q844, Q845, Q846, Q847, Q848, Q849, Q850, Q851, Q852, Q853, Q854, Q855, Q856, Q857, Q858, Q859, Q860, Q861, Q862, Q863, Q864, Q865, Q866, Q867, Q868, Q869, Q870, Q871, Q872, Q873, Q874, Q875, Q876, Q877, Q878, Q879, Q880, Q881, Q882, Q883, Q884, Q885, Q886, Q887, Q888, Q889, Q890, Q891, Q892, Q893, Q894, Q895, Q896, Q897, Q898, Q899, Q900, Q901, Q902, Q903, Q904, Q905, Q906, Q907, Q908, Q909, Q910, Q911, Q912, Q913, Q914, Q915, Q916, Q917, Q918, Q919, Q920, Q921, Q922, Q923, Q924, Q925, Q926, Q927, Q928, Q929, Q930, Q931, Q932, Q933, Q934, Q935, Q936, Q937, Q938, Q939, Q940, Q941, Q942, Q943, Q944, Q945, Q946, Q947, Q948, Q949, Q950, Q951, Q952, Q953, Q954, Q955, Q956, Q957, Q958, Q959, Q960, Q961, Q962, Q963, Q964, Q965, Q966, Q967, Q968, Q969, Q970, Q971, Q972, Q973, Q974, Q975, Q976, Q977, Q978, Q979, Q980, Q981, Q982, Q983, Q984, Q985, Q986, Q987, Q988, Q989, Q990, Q991, Q992, Q993, Q994, Q995, Q996, Q997, Q998, Q999, Q1000.







TOPVIEW
(POWER PACK
COMPARTMENT)



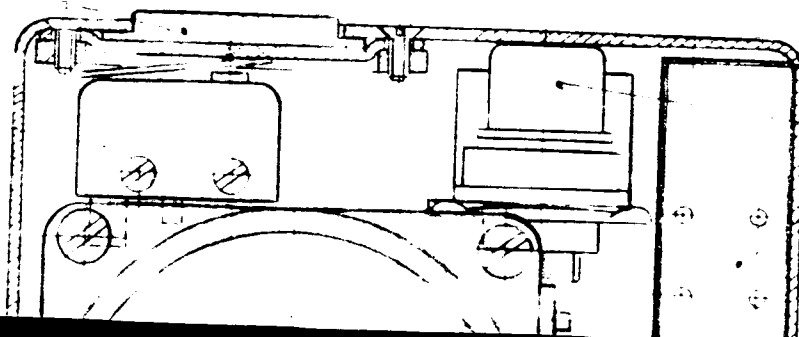
TOPVIEW
DOSIMETER ASSLY

PUSH
BUTTON

030 MAX.

SUB-MINIATURE
SWITCH
#A5-11/T2

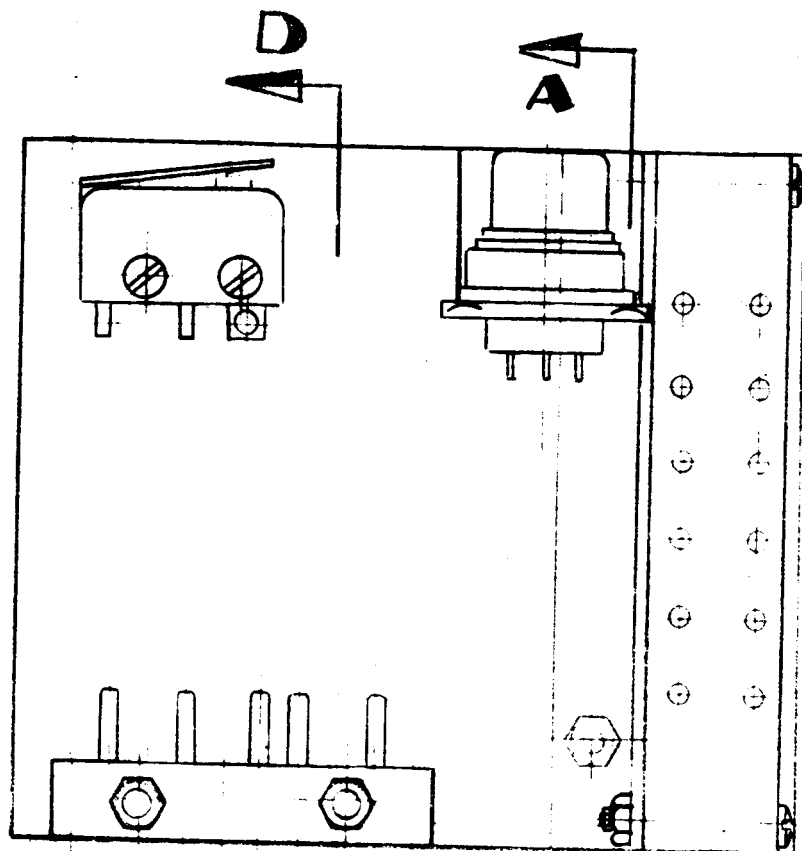
CYCLE
TIMER



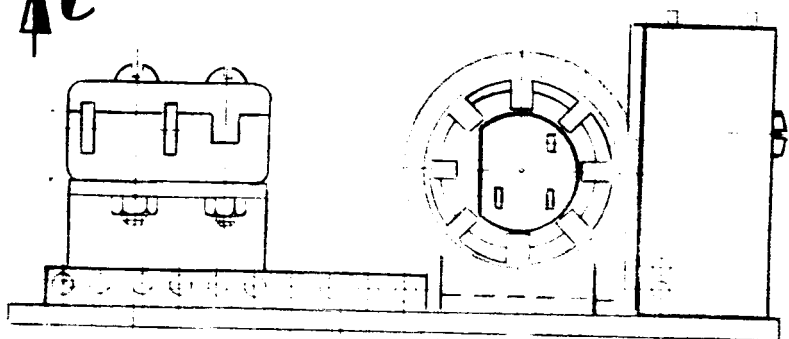
6

DETECTOR
ASSEMBLY
AM-LIFE

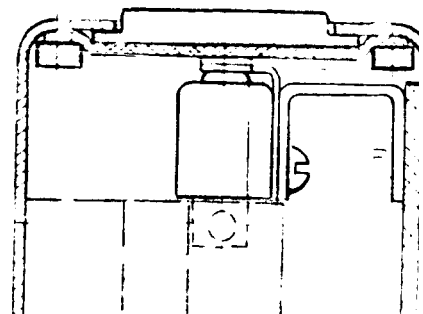
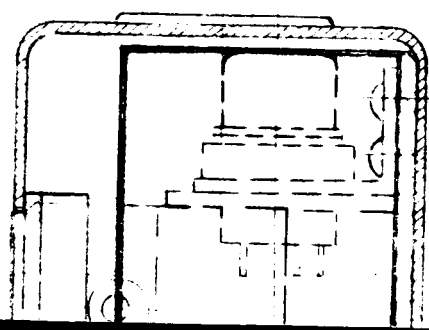
2



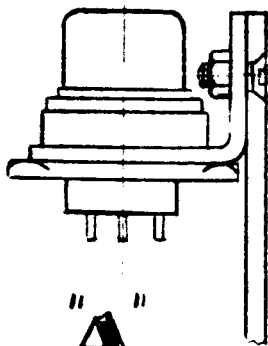
↑C



VIEW "C"



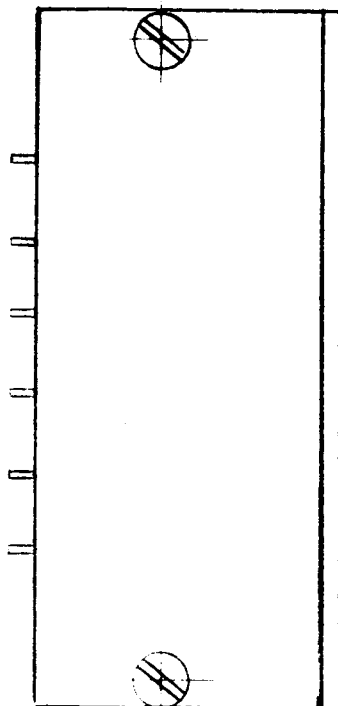
3



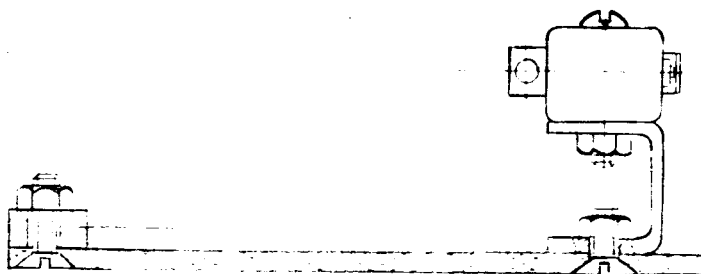
"A"

B
A

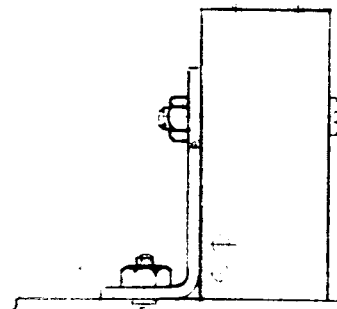
CIRCUIT
ASSLY



VIEW "B"



"D"



3.00

POWER
SUPPLY
COMPARTMT.

BATTERY
COMPARTMTS.

BALL
PLUG, 51

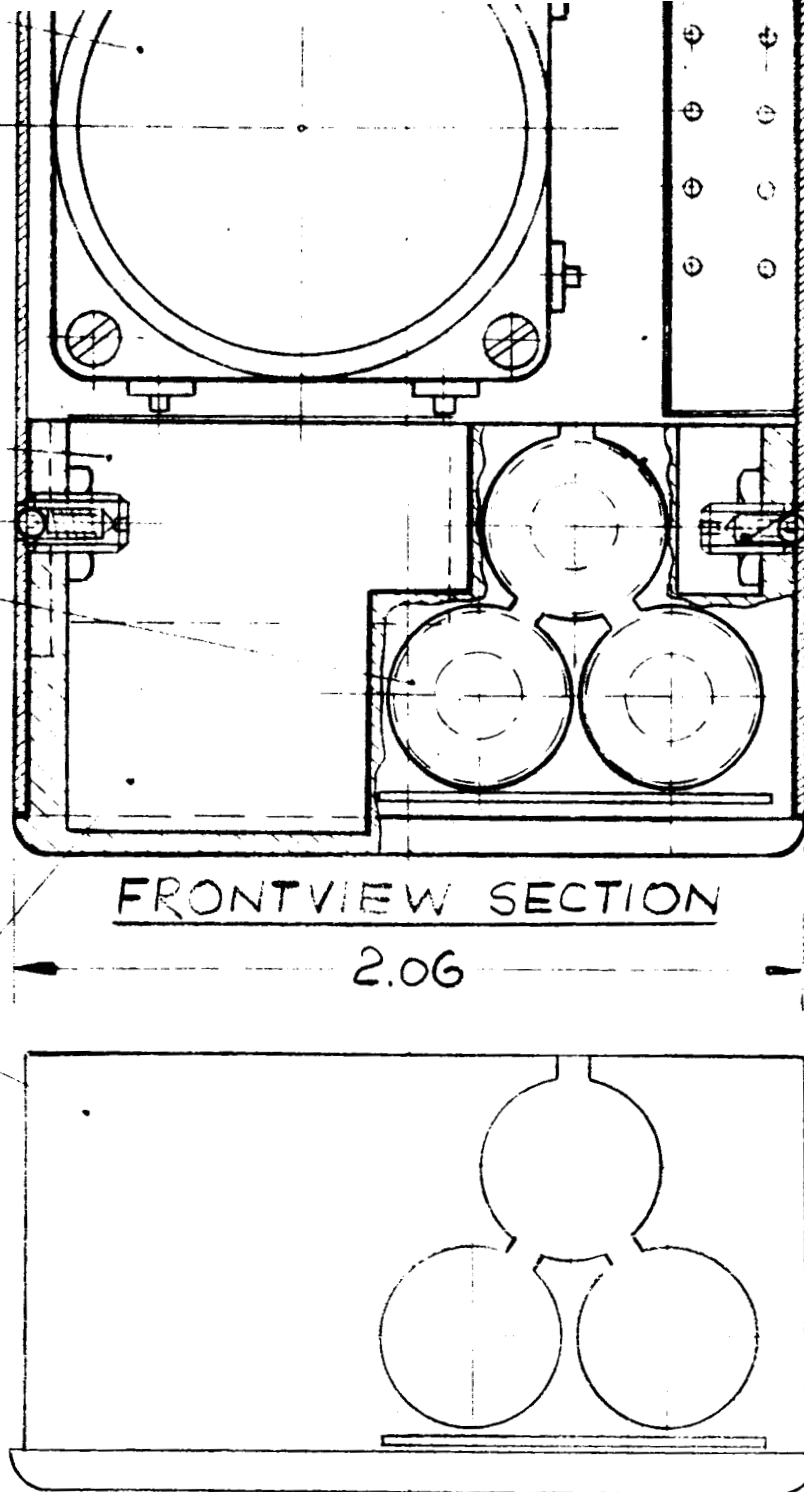
FRONTVIEW SECTION

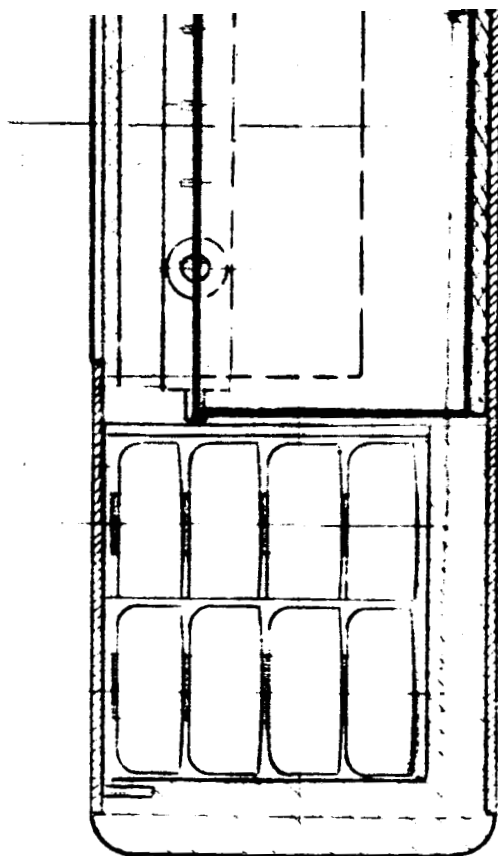
2.06

POWER PACK
COMPARTMENT

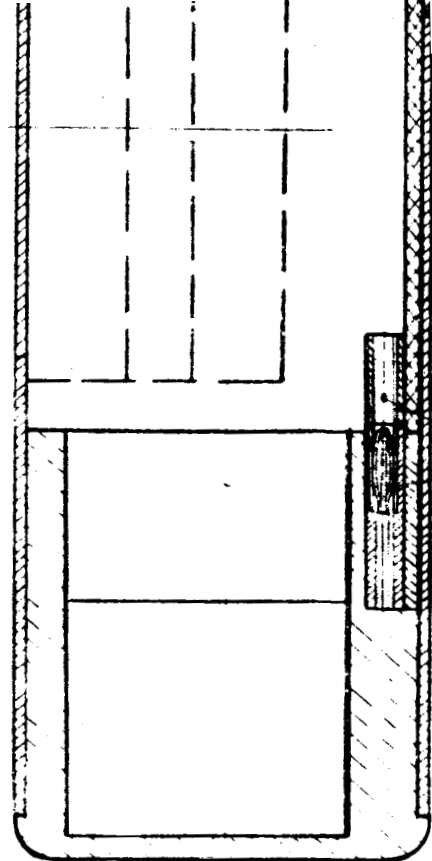
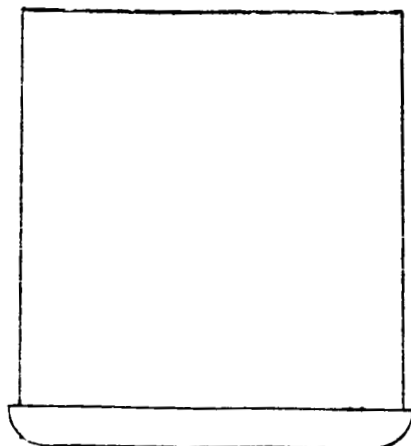
1.10

4





SIDE VIEW
SECTION



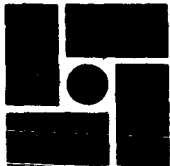
SIDE VIEW
SECTION

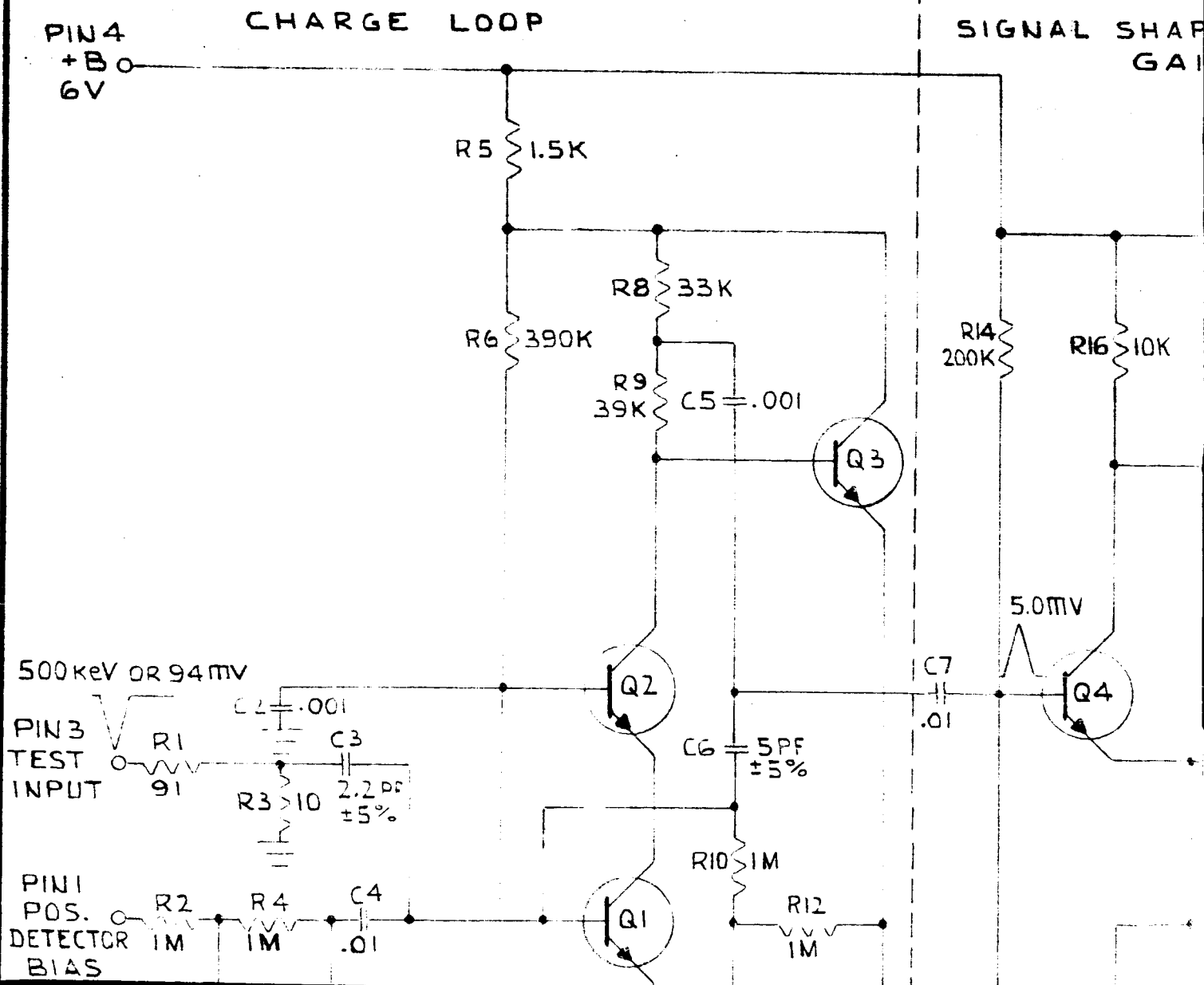
| | |
|----------------------------|--|
| REQD. | |
| | |
| | |
| | |
| DRAWN | |
| CHECKED | |
| APPROVED | |
| UNLESS OTHERWISE SPECIFIED | |
| DIMENSIONS ARE IN INCHES | |
| TOLERANCES ARE: | |
| 3 PLACE DEC 2 F | |
| ± | |

AMPLIFIER BRACKET

STRIP-
CONNECTOR

6

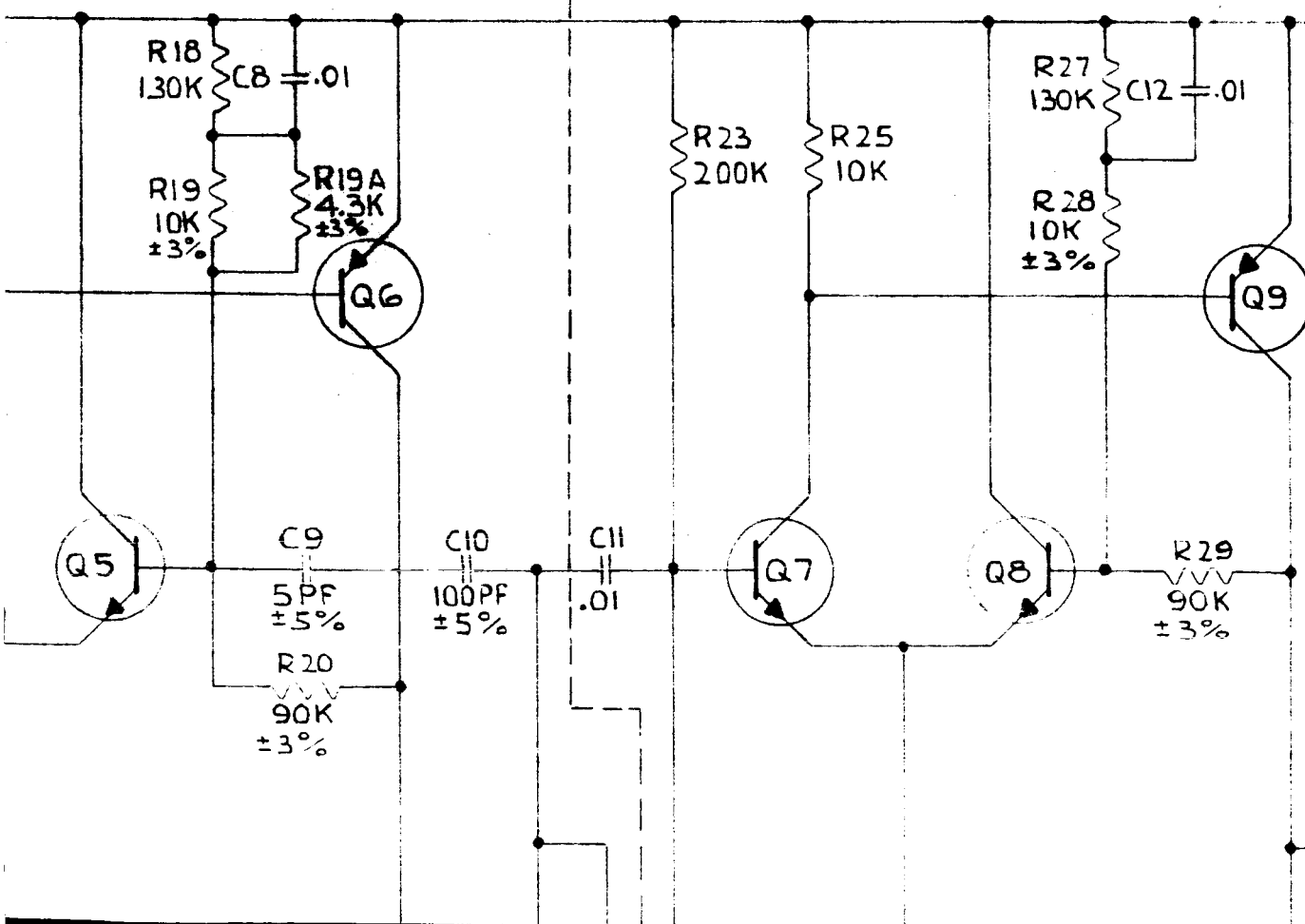
| PART NO. | DESCRIPTION | ITEM |
|--|--|---|
| LIST OF MATERIALS | | |
| | <div data-bbox="356 1073 526 1239"></div> <div data-bbox="557 1122 1202 1159">SOLID STATE RADIATIONS, INC.</div> <div data-bbox="573 1166 1198 1198">2261 S. CARMELINA AVE., LOS ANGELES, CALIFORNIA</div> | |
| | <div data-bbox="393 1284 1155 1430"><u>MECHANICAL LAYOUT</u> <u>PROTON DOSIMETER</u></div> | |
| <div data-bbox="38 1430 286 1573">OTHERWISE SPECIFIED IN INCHES PLACE DEC ANGLES ± 1 ±</div> | <div data-bbox="330 1490 626 1573">SCALE 2x 2-26-65</div> | <div data-bbox="702 1495 1268 1549">C1573MIE54-65</div> |



2

ING AMPLIFIER
N=10

1ST
VOLTAGE AMPLIFIER
GAIN=10



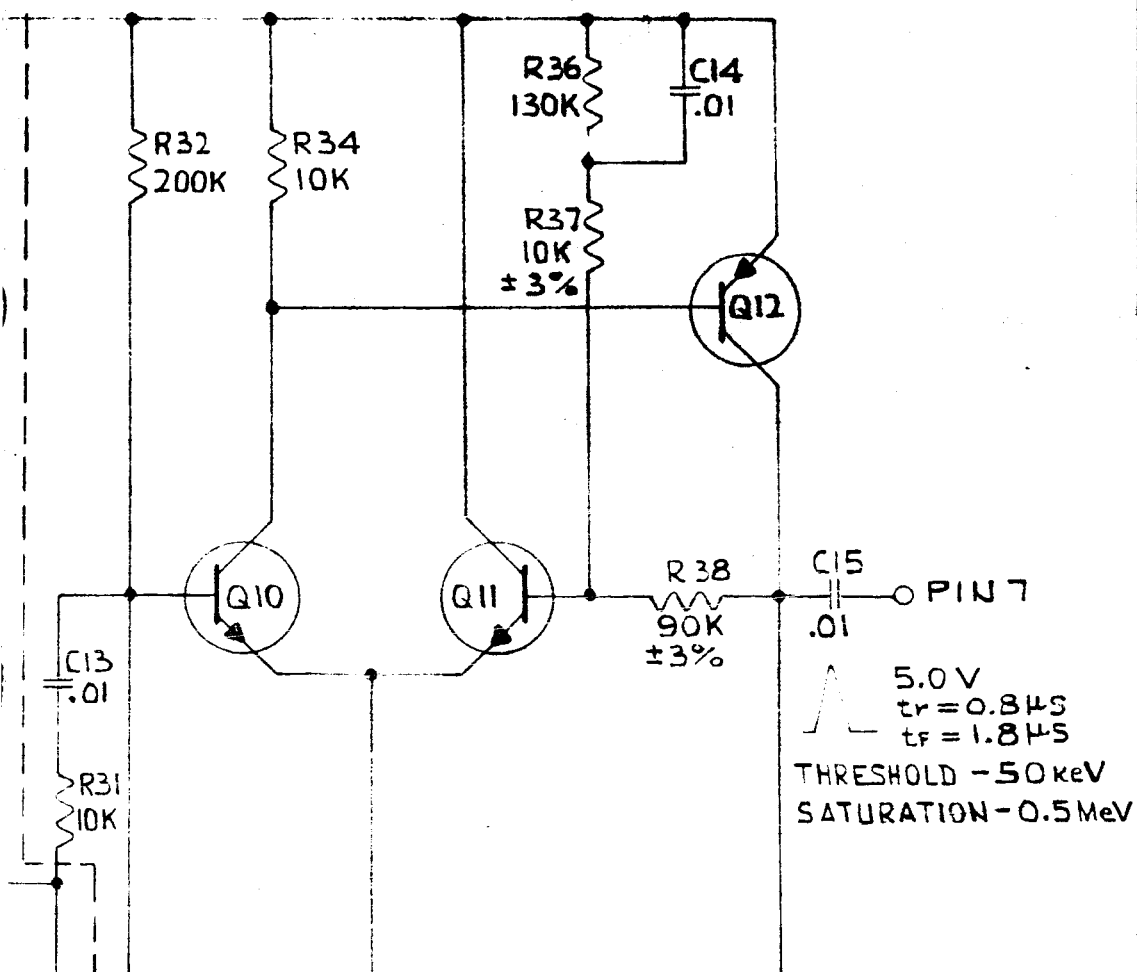
NO.

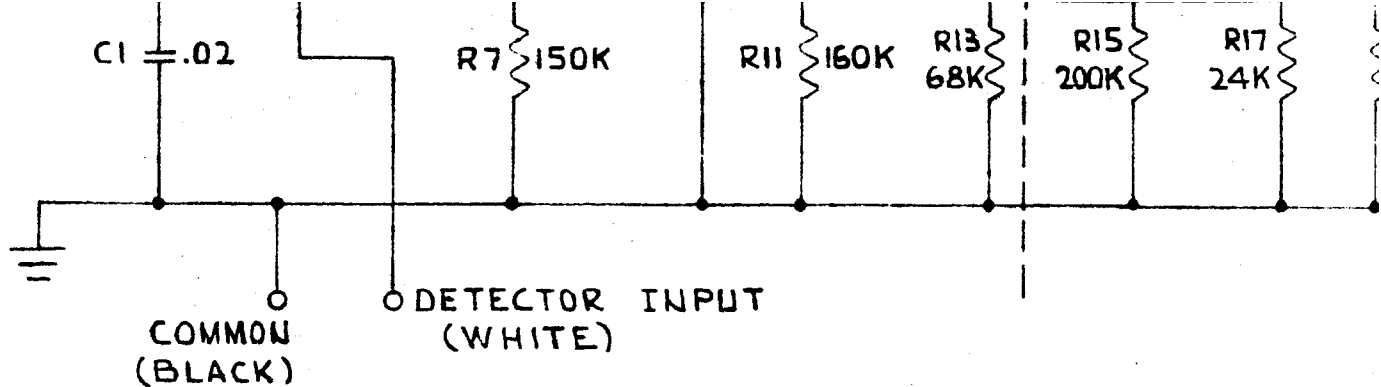
REVISION

DATE

3

2ND
VOLTAGE AMPLIFIER
GAIN = 10





UNLESS OTHERWISE NOTED:

1. ALL CAPACITORS IN MFD.
2. ALL RESISTORS IN OHMS $\pm 10\%$
3. Q1, Q2, Q3, Q4, Q5, Q7, Q8, Q10, Q11 - 2N2388 ; Q6, Q9, Q12 - 2N2907

K17A
24K

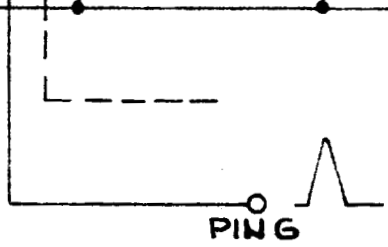
R21
10K

R22
10K
 $\pm 5\%$

R24
200K

R26
24K

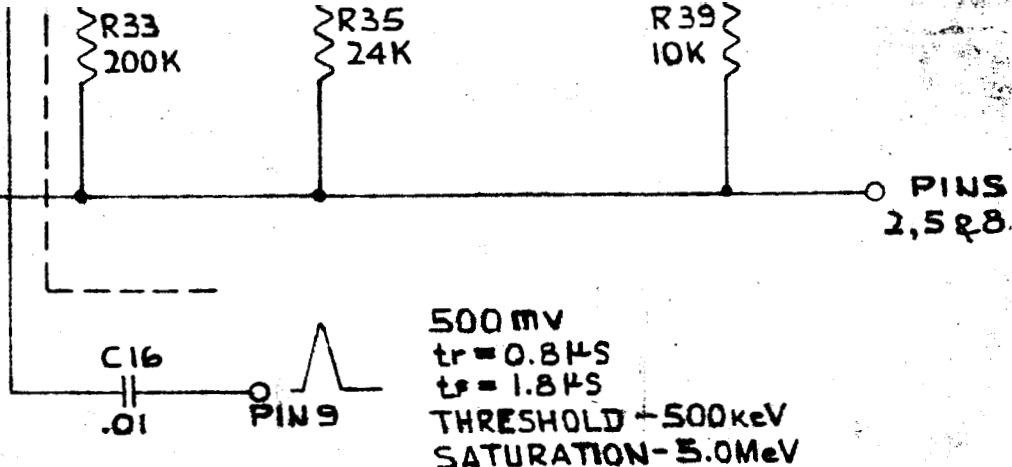
R30
10K




50 mV
 $t_r = 0.6 \mu s$
 $t_f = 2.5 \mu s$
THRESHOLD - 5.0 MeV
SATURATION - 50 MeV

| REQD. | PART NO. |
|-----------------------------|----------|
| | |
| DRAWN V. BER | |
| CHECKED <i>[Signature]</i> | |
| APPROVED <i>[Signature]</i> | |
| UNLESS OTHERWISE | |
| DIMENSIONS ARE IN IN. | |
| TOLERANCES ON | |
| 3 PLACE DEC 2 PLACE DEC | |
| \pm | \pm |

5



| D. | | DESCRIPTION | ITEM |
|--------------------------|--|---|--|
| LIST OF MATERIALS | | | |
| | |  SOLID STATE RADIATIONS, INC. 2261 S. CARMELINA AVE., LOS ANGELES, CALIFORNIA | |
| 6.9.65 | | AMPLIFIER FOR SUB MINIATURE PROTON DOSIMETER | |
| 6/10/65 | | | |
| 6/10/65 | | | |
| E SPECIFIED CHES | | | |
| C ANGLES ± | | SCALE _____ | C1502E1554-65 <div style="float: right; font-size: 2em; font-weight: bold;">6</div> |